## REMARKS/ARGUMENTS

Claims 1-10 and 12-27 remain in this application. Claims 1 has been amended. Claim 11 has been cancelled by a previous amendment.

**Claims 1, 4, 6-8, 13, 15, 17, 18 and 25-27 are rejected under 35 USC 103(a) as being unpatentable over Kawanishi et al (US 6,404,966 B1).**

**I.** Claim 1 has been amended to state that the band gap structure has non-circular holes. This amendment is supported, for example, by Fig. 7 of the Applicants' specification. Such band gap structure is not disclosed by the Kawanishi et al (US 6,404,966 B1) reference. Accordingly, claim 1 and its dependent claims 4, 6-8, 13, 15, 17, 18 are not obvious over this reference.

**II.** Furthermore, Claim 1 states that "the optical energy is guided in a mode having a nonlinear refractive index of less than about $10^{-18}$ $cm^2/W$." As discussed in the previous amendment, this parameter contributes to the low loss and is not taught or disclosed by the cited reference. In fact, pg. 7, paragraph [0033] of the Applicants specification discloses that in conventional fibers the guided modes have effective nonlinear refractive indices $n_2$ ranging from $2x10^{-16}$ $cm^2/W$ to $4x10^{-16}cm^2/W$ while some of the Applicants claims call for it being less than $10^{-18}$ $cm^2/W$ . (This is at least a factor of 10 different (or about 20 times less) than that of the conventional fibers.)

On page 2 of the Office Action dated 3/6/2006 the Examiner stated that the "references teach achieving this index by using air filled holes to guide the optical energy in PBG fibers. Applicants own disclosure identifies the nonlinear index of air to be $2.9x10^{-19}cm^2/W$ which is within the claimed range."

Applicants respectfully traverse the grounds for this rejection, for the following reasons:

Applicants understood the Examiner's statement as saying that: (i) the references teach fibers with hollow (air filled) cores and that air has a nonlinear refractive index of 2.9 $x10^{-19}$ $cm^2/W$, and (ii) thus it should be obvious that a mode propagating in such fiber will have an effective nonlinearity of 2.9 $x10^{-19}$, which is less than about $10^{-18}$ $cm^2/W$. This conclusion can be logically reached if and only if *all* of the light is carried in the hollow-core region. However, this is not how FBG fibers work. (However, if Applicant's misunderstood what Examiner is saying, it is requested that the Examiner provide a more detail explanation of the rejection.)

Applicants disagree with this assumption and suggest that it is not at all obvious that hollow-core fibers support a mode with such low nonlinearity (less than $10^{-18}$ $cm^2/W$). A recent publication (see enclosed) by C. J. Hensley, D. G. Ouzounov, A. L. Gaeta, N. Venkataraman, M. T. Gallagher, and K. W. Koch, "Silica-glass contribution to the effective nonlinearity of hollow-core photonic band-gap fibers," Opt. Express 15, 3507-3512 (2007)) teaches:

> "The optical field is primarily localized in the air core, but since the nonlinear refractive index of glass is roughly 1000× larger than that of air, it is not obvious which medium dominates the effective nonlinearity of the fiber. It was shown [5] that the effective nonlinearity of the fundamental mode of the fiber described in Ref. 3 is approximately equal to that of the air in the fiber core. Alternatively, theoretical analysis of other commercially available HC-PBGFs [6, 7] concluded that glass and air regions have comparable contributions to the total nonlinearity. Lægsgaard *et al.* [14] showed theoretically that the fraction of light that resides in the silica regions, and thus the glass contribution to total nonlinearity depends strongly on the air-filling fraction." (Emphasis added.)

Thus, it is clear that the presence of an air core alone is insufficient in determining the nonlinearity of the refractive index of the optical mode in the fiber waveguide.

A simple calculation illustrates the problem:

- Nonlinear refractive index of air:

$$n_{2,air} = 2.9 \times 10^{-19} \text{ cm}^2/\text{W} \quad (1)$$

- Nonlinear refractive index of silica:

$$n_{2,glass} = 2.6 \times 10^{-16} \text{ cm}^2/\text{W} \quad (2)$$

If we consider the nonlinear refractive index to be a simple weighting of the fraction of the optical intensity in the glass (we will denote this fraction as f) and the fraction intensity of the light in the air (thus, 1-f) we find:

$$n_2 = f \times n_{2,glass} + (1-f) \times n_{2,air} \quad (3)$$

Claim 1 sets the limit on the nonlinear refractive index $n_2$ of the optical mode to be less than $10^{-18}$ cm$^2$/W. From equation (3) we must then have:

$$2.6\times10^{-16} f + 2.9\times10^{-19} (1-f) < 10^{-18}, \quad (4)$$

or:

$$\mathbf{f<0.11\%.} \quad (5)$$

Thus, less than 0.11% of the light is propagating through the glassy region of the cladding. Those skilled in the art recognize that it is not obvious that one can achieve less than 0.11% overlap of the light in the glass, because the optical mode always has some significant overlap with the cladding (or else one could remove the cladding with no effect).

It was Applicants who taught that it *is* possible to have a photonic band gap fiber that guides an optical mode (guided by a band-gap cladding) such that the optical energy is guided in a mode having a nonlinear refractive index of less than about $10^{-18}$ cm$^2$/W i.e.- it was applicants who taught that it *is* possible to have a mode that propagates with very little overlap with such silica portion of the cladding. Applicants do not find that the references (from *Kawanishi et al*, *Libori et al* and *Fajardo et al*) enable or teach or suggest how to achieve such small overlap with the glass in their structures, or that such small overlap is even possible. A recent (see enclosed) reference (J. Lægsgaard, N. A. Mortensen, J. Riishede, and A. Bjarklev, "Material effects in air-guiding photonic bandgap

fibers," J. Opt. Soc. Am. B **20**, 2046-2051 (2003)) has the following discussion of overlap with the glass for air holes of diameter *d* separated by a pitch Λ:

> For the design with $d/\Lambda = 0.88$, where 7–9% of the field energy is in silica, the material dispersion ranges between ~0 and -200 ps/nm/km, whereas for the design with $d/\Lambda = 0.95$ and only 2–3% of the field energy in silica, the material contribution to the GVD ranges between -50 and 50 ps/nm/km.

These ranges (7% to 9% and 2% to 3 %) are much larger than 0.11% that corresponds to the non-linear refractive index of nonlinear refractive index of less than about $10^{-18}$ $cm^2/W$ called for in claim 1 and its dependent claims.

The mode overlap with the glass decreases as the air-filling fraction is increased. With circular holes this is accomplished by increasing the diameter *d* of the air holes. However, Applicants' calculations show that for circular holes (such as those shown by the cited references-i.e., *Kawanishi et al*, *Libori et al* and *Fajardo et al* references), an overlap of greater 1.7% (see calculated data in Fig. 1, below) between the optical mode and silica based cladding is achieved when the air holes just touch, $d/\Lambda = 1.00$.

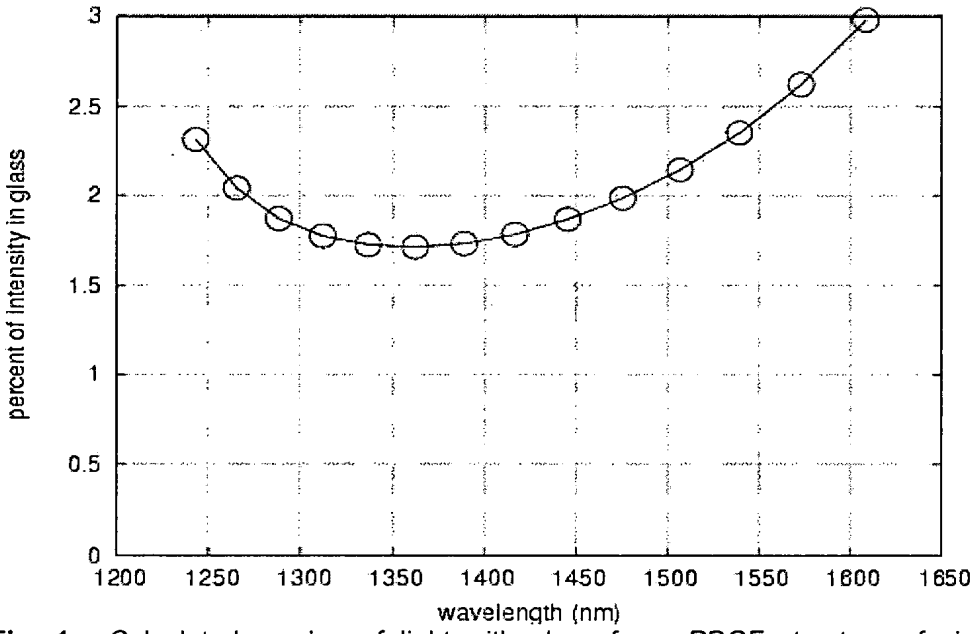


**Fig. 1.** Calculated overlap of light with glass for a PBGF structure of circular air holes (refractive index n=1) in silica (refractive index n=1.45), air-hole diameter of d=3.5 μm, and hole-to-hole spacing or pitch of Λ=3.5 μm. The holes are just touching.

This value is insufficient to reach the low nonlinearity claimed by Applcants. In fact this value is about 10 times larger than the required overlap calculated above, and Applicants do not believe that a further reduction of 10X is obvious or enabled by this reference. Any further increase in the size of circular holes without the change in pitch (hole separation) leads to a **disconnected unphysical structure.**

Applicants achieved small overlap between the guided mode and the cladding of the PBG fiber, for example, by using structures with *non-circular* air holes (shown in our Figure 7 in original patent application) and/or very large airfilled ratious, which structures are not disclosed by the cited reference of *Kawanishi (nor is it disclosed by Libori et al* or *Fajardo et al).* Accordingly, claim 1 is note obvious over the cited reference(s).

Claims 4, 6-8 13, 15, 17 and 18 depend from claim 1 as their base claim and, therefore, explicitly incorporate the language of claim 1. Accordingly Applicants respectfully submit that claims 1, 4, 6-8 13, 15, 17 and 18 are not obvious over the Kawanishi reference.

**III.** Claims 25-27 (and 13) state that the "optical fiber is configured to support a temporal soliton having a peak power of greater than about 1 MW". Such fiber is not disclosed by the Kawanishi reference, and the Kawanishi reference provides no incentive for having a fiber with this characteristics. Accordingly, claims 13 and 25-27 are not obvious over this reference.

The Examiner, in replying to Applicants' previous response stated that "Kawanishi et al also teach that the optical fiber can be used to transmit pulses (see column 1, lines 60-63). As discussed above, the non-linear refractive index results in minimal pulse spreading. Therefore, the pulse will retain its shape. Pulses such as these are solitons. One of ordinary skill in the art recognizes the benefit and desirability of high power

signals. It would be obvious to one of ordinary skill in the art at the time of invention to use an optical soliton pulse having a peak power of 3MW ..."

Applicants respectfully disagree with this statement for the following reasons:

Retaining its shape is a necessary but *not sufficient* condition to define a soliton. The term soliton was coined in 1965 to reflect the particlelike nature of solitary waves that remain intact even after mutual collision. The following excerpt is from an authoritative source (G. Agrawal, "Fiber-Optic Communication Systems," (Wiley & Sons, New York, 1997) p. 468) on optical fiber communications (also enclosed):

> The existence of fiber solitons is the result of a balance between *group-velocity dispersion* (GVD) and *self-phase modulation* (SPM), both of which, as discussed in Sections 2.4 and 5.2, limit the performance of fiber-optic communication systems when acting independently on optical pulses propagating inside the fiber. One can develop an intuitive understanding of how such a balance is possible by following the analysis of Section 2.4. As shown there, the GVD broadens optical pulses during their propagation inside the fiber except when the pulse is initially chirped in the right way (see Fig. 2.12). More specifically, a chirped pulse can be compressed during the early stage of propagation whenever the GVD parameter $\beta_2$ and the chirp parameter C happen to have opposite signs, so that $\beta_2 C$ is negative. SPM, resulting from the intensity dependence of the refractive index, imposes a chirp on the optical pulse such that $C > 0$. Since $\beta_2 < 0$ in the 1.55-pm wavelength region, the condition $\beta_2 C < 0$ is readily satisfied. Moreover, since the SPM-induced chirp is power dependent, it is not difficult to imagine that under certain conditions, SPM and GVD may cooperate in such a way that the SPM-induced chirp is just right to cancel the GVD-induced broadening of the pulse. The optical pulse would then propagate undistorted in the form of a soliton.

As mentioned above, in optical fibers there <u>are two main forces that cause pulses to spread: self-phase modulation (SPM) and group-velocity dispersion</u> (often referred to simply as dispersion). An important note is that group-velocity dispersion has several sources: material dispersion, waveguide dispersion, modal dispersion and profile dispersion (see G. Agrawal, "Fiber-Optic Communication Systems," (Wiley & Sons, New York, 1997) pp. 39-49, enclosed). A fiber with an air core has near-zero material dispersion but may have significant waveguide, modal and profile dispersion.

One might expect that an optical pulse traveling through a medium with low nonlinearity would not spread. However, this argument does not consider the spreading due to group-velocity dispersion. None of the cited reference addresses or discusses this issue. Accordingly, Applicants' claims are unobvious over these references.

Applicants are claiming an optical fiber and optical fibers inherently have at least the waveguide form of group-velocity dispersion referred to above. Even if it is possible to eliminate the other forms of dispersion, it is impossible to eliminate *waveguide* group-velocity dispersion at all wavelengths in an optical waveguide. Typically there may be one or more discrete zero-dispersion wavelengths in an optical waveguide, however, by analytic continuation one may not have zero dispersion over a continuous range of wavelengths unless dispersion is zero everywhere (and this is impossible in a waveguide).

A pulse in time implies a finite spectral width and thus, from the argument above, must include wavelengths at which dispersion is non-zero. Thus such a pulse will spread due to dispersion unless balanced by another mechanism.

Thus, it is not sufficient to have only low nonlinearity or only low dispersion to support a soliton pulse. The cited reference(s) teach nor make obvious the formation of solitons in hollow-core fibers. The Libori et al reference mentions solitons in the context of conventional fibers (column 1 lines 13-20) but it is not obvious, for the reasons explained above, that this concept can be extended to hollow-core fibers, or band-gap fibers, and the recited reference(s) do not suggest that this can be done. The extension to soliton propagation in hollow-core fibers is not obvious. For instance, the examiner has argued that it is obvious that hollow-core fibers have low nonlinearity because they have a low nonlinearity core. This is logically true only if all of the light is carried in the core region. Let us suppose, arguendo, that is true—then we propose to evacuate such a fiber. Now, in the absence of a core material the core nonlinearity is zero. However, as discussed above, such a fiber will not support a soliton because there is no nonlinearity to balance the waveguide dispersion. Fortunately the "obvious" argument that all

of the light is carried in the hollow region is flawed and Applicants discovered, as taught in the present application, that photonic band-gap fibers can indeed support solitons.

Accordingly, claims 13, and 25-27 are not unpatentable over Kawanishi et al (US 6,404,966 B1).

It is noted that Applicants balanced the pulse spreading by designing fibers that use SPM, a result of the fiber nonlinearity, to cancel the inherent group-velocity dispersion of the fiber. This nonlinear effect leads to a chirp of the optical pulse as described in the reference above. The optical fiber nonlinearity is always greater than zero as a result of the intrinsic properties of the glass and this sign determines the nature of the pulse spreading (leads to $C>0$, longer wavelengths move ahead of the shorter wavelengths). This nonlinear chirping is proportional to the intensity of the optical pulse. To balance the spreading from this chirping Applicants' waveguide fibers have the group-velocity dispersion in the fiber which has opposite effect, such that shorter wavelengths travel faster than longer wavelengths. If the fiber is designed correctly *and* the pulse intensity is correct, it is possible to achieve a balance over an extended wavelength range that includes the pulse spectrum. In such a fiber, nonlinear SPM cancels the anomalous group-velocity dispersion and the optical pulses can propagate without spreading, giving a rise to solitons, as disclosed and claimed by Applicants. However, this is not an obvious solution, and the air filled cores, generally do not support solitons, nor make it obvious on how to do it.

**Claims 1-3, 5, 6-10, 13, 14, 16-18 and 25-27 are rejected under 35 USC 103(a) as being unpatentable over Libori et al (US 6,792,188 B2).**

**I.** Claims 1-3, 5, 6-10, 13, 14 and 16-18 call for a bandgap fiber having a core region surrounded by a "cladding region including a photonic band gap structure with non-circular holes, the optical energy having a wavelength within the photonic band gap of the photonic

band gap structure". Such fiber is not disclosed by the Libori reference. Plase note that although Fig. 34 of Libori shows a microstructured fiber, this fiber is not a bandgap fiber because the fiber of Fig. 34 has solid core with an index of referaction higher than the surrounding structure.

**II.** Furthermore, as discussed above, Applicant's claims 1-3, 5, 6-10, 13, 14 and 16-18 specify that "the optical energy is guided in a mode having a nonlinear refractive index of less than about $10^{-18}$ $cm^2/W$", and this feature is not shown, disclosed or discussed by the Libori reference. As shown above, one of skill in the art will recognise that the nonlinear refractive index of less than about $10^{-18}$ $cm^2/W$ corresponds to a fiber that has a very small overlap between the mode and the fiber cladding structure. This feature is not obvious, because no cited references taught or disclosed that it is even possible to achieve the minimal required overlap between the optical mode and the cladding structure surrounding the core (less than a fraction of 1%), and no cited reference shows any embodiments capable of achieving it.

More specifically, the Examiner pointed that "Labori et al teach that PBG structure can include air holes. Air has a nonlinear refractive index of $2.9x10^{-19}$ $cm^2/W$ which is within the claimed range." As discussed above, the presence of air alone is not enough to bring the nonlinear refractive index of the guided mode within the range claimed by the applicants. The Libori reference does not disclose, teach, or suggest what is required to achieve the low non-linearity claimed by the Applicants. The Libori reference also does not provide any enabling examples that teach how to achieve the "optical energy is guided in a mode having a nonlinear refractive index of less than about $10^{-18}$ $cm^2/W$".

**III.** Morever, as discussed in the previous Response, although Libori makes a statement that a low loss fiber is desirable and can be achieved with PBG structure, Libori does not define what is meant by a "low loss", nor provides an enabling embodiment of the PBG structure that has the losses in the Applicant's claimed range. A mere statement that something is desirable, without a way of how to achieve such a

result, does not constitute an enabling disclosure. Also, a mere statement that something is desirable, does not make it achievable to one of ordinary skill in the art. The general conditions for achievement of very low loss (e.g., less than 50 dB/km, or less than 20 dB/km) for PBG fibers were disclosed by the Applicants and were not known to one of ordinary skill in the art, nor were disclosed by the Libori reference, although the was a long felt need to have a fiber with these characteristics.

**IV.** Finally, as stated above, Claims 25-27 call for the "optical fiber is configured to support a temporal soliton having a peak power of greater than about 1 MW". Such fiber is not obvious for the reasons discussed above, is not disclosed by the Liborui reference, and the reference provides no teaching that would lead someone to a fiber with this characteristics.

Accordingly, claims 1-3, 5, 6-10, 13, 14, 16-18 and 25-27 are not unpatentable over Libori, et al.

**V.** Furthermore, the Examiner (see pg. 5 of the Office Action) stated that figures 1 and 2 of the Libori reference teach PGB structure. However, since these figures clearly show a solid core, the fibers of Libori's Figures 1 and 2 can not be PBG fibers. The Examiner also referred Applicants to Fig. 5 of the Libori reference. Again, since this figure clearly shows a solid core, the fiber of Libori's Figure 5 can not be a PBG fiber (it will not have a photonic band gap).

**Claims 1, 4, 6, 7, 12, 15, 19, 20, 22 and 23 are rejected under 35 USC 103(a) as being unpatentable over Fajardo et al (US 6,444,133 B1).**

**I.** Claims 1, 4, 6, 7, 12, 15, 19 and 20 call for an optical fiber that guides the optical energy in a mode having a nonlinear refractive index of less than about $10^{-18}$ $cm^2/W$. As explain above, the fact that a fiber (such as Fajaro fiber) has a hollow core, doe not mean that the fiber satisfies this condition. As known to one skill in the art, because the mode propagates

in the core and in partially in the cladding. Accordingly, because the nonlinear refractive index of the mode depends on the refractive index of the core and that of the cladding, claims are claims 1, 4, 6, 7, 12, 15, 19 and 20 are not obvious over the Fajardo reference. It is noted that the Fajardo reference does not disclose FBG fibers that are capable of satisfying this condition, nor teach or suggest that the claimed condition can be satisfied, nor teach, suggest or discuss any fibers capable of guiding the modes such that the overlap between the mode and the cladding is only a fraction of 1%.

Claim 20 depends from claim 19 as its base claim and is even more stringent, requiring a factor of 2 improvement –i,e., it calls for "optical signal is guided in a mode having a nonlinear refractive index of less than about $5 \times 10^{-19}$ $cm^2/W$ ". No such fibers are shown or even suggested by the Fajardo or any other cited references.

Claims 22 and 23 depend from claim 19 as their base claim, and therefore explicitly incorporate a subject matter of claim 19. Therefore, claims 22 and 23 are not obvious over the Fajardo for the same reasons that claim 19 is not obvious over this reference.

**II.** With regard to claims 22 and 23, the Fajardo reference does not disclose the fiber with ether a loss of a loss of less than about 300 dB/km, less than 50 dB/km, etc, or that has a nonlinear refractive index of less than about $10^{-18}$ $cm^2/W$, or less than $5x10^{-19}$ $cm^2/W$. The low loss feature (not disclosed by the Fajardo reference) in combination with the low nonlinearity (also not disclosed by the reference), where the claimed nonlinear refractive index at least one to two orders of magnitude smaller than similar known fibers (and certainly not within general ranges disclosed by prior art fiber references), make applicants claims unobvious 22 and 23 over Fajardo, and other the cited references.

**Claims 21 and 24 are rejected under 35 USC 103(a) as being unpatentable over Fajardo et al (US 6,444,133 B1) as applied to claims 1, 4, 6, 7, 12, 15 19, 20, 22 and 23 above, and further in view of Libori et al (US 6,792,188 B2).**

Claims 21 and 24 depend from claim 19 as their base claim, and further call for solitons.

Claims 21 and 24 being dependent claims explicitly incorporate a subject matter of claim 19. Therefore, claims 22 and 23 are not obvious over the Fajardo for the same reasons that claim 19 is not obvious over this reference.

Furthermore, as described above, just because PBG fiber has an air core does not mean that it can support soliton propagation, because the fiber also has a cladding, and there is interaction between the mode and the cladding. Futhermore, column 1, lines 13-20 of Libori are directed to "conventional" fibers, and not to PBG fibers. Libori does not teach that any of its disclosed embodiments of PBG fibers supports solitons. The Examiner stated (see pg. 7 of the Office Action) that "It would have been obvious to one of ordinary skill to modify the Fiber of Fajardo et al to support solitons as taught by Libori et al". However, the Libori refernce does not teach how to make such modification.

**Conclusions**

Based upon the above amendments, remarks, and papers of records, applicant believes the pending claims of the above-captioned application are in allowable form and patentable over the prior art of record. Applicant respectfully requests that a timely Notice of Allowance be issued in this case.

Applicant believes that no extension of time is necessary to make this Reply timely. Should applicant be in error, applicant respectfully requests that the Office grant such time extension pursuant to 37 C.F.R. § 1.136(a) as necessary to make this Reply timely, and hereby authorizes the Office to charge any necessary fee or surcharge with respect to said time extension to the deposit account of the undersigned firm of attorneys, Deposit Account 03-3325.

Please direct any questions or comments to Svetlana Z. Short at 607-974-0412.

Respectfully submitted,

DATE: 5/10/07

Svetlana Z. Short
Attorney for Assignee
Registration Number: 34,432
Corning Incorporated
SP-TI-03-1
Corning, NY 14831
Phone: 607-974-0412

# Material effects in air-guiding photonic bandgap fibers

**Jesper Lægsgaard**

*Research Center, Technical University of Denmark, DK-2800 Kongens Lyngby, Denmark*

**Niels Asger Mortensen**

*Crystal Fibre A/S, Blokken 84, DK-3460 Birkerød, Denmark*

**Jesper Riishede and Anders Bjarklev**

*Research Center, Technical University of Denmark, DK-2800 Kongens Lyngby, Denmark*

Received February 7, 2003; revised manuscript received May 15, 2003

The waveguiding properties of two silica-based, air-guiding photonic bandgap fiber designs are investigated with special emphasis on material effects. The nonlinear coefficients are found to be 1–2 orders of magnitude smaller than those obtained in index-guiding microstructured fibers with large mode areas. The material dispersion of silica makes a significant contribution to the total chromatic dispersion even though less than 10% of the field energy is located in the silica regions of the fibers. These findings suggest that dispersion engineering through the choice of base material may be a possibility in this type of fiber. © 2003 Optical Society of America

*OCIS codes:* 060.2310, 060.2400, 260.2030.

## 1. INTRODUCTION

Photonic bandgap (PBG) fibers guiding light in a hollow core surrounded by a cladding structure with a bandgap at a refractive index below the light line have attracted considerable attention since their first experimental demonstration by Cregan *et al.*[1] Such fibers have been proposed as candidates for highly linear and possibly low-loss transmission fibers,[1] devices for particle transport,[2] dispersion compensation,[3] and gas nonlinearity experiments.[4] In contrast to conventional fibers, the useful wavelength range is not limited by the absorption loss and nonlinearity of the base material. The recent fabrication of silica-based, air-guiding PBG fibers with attenuation coefficients below 30 dB/km over a considerable wavelength range[5] opens up a wide range of practical applications.

It is usually assumed that the influence of the base material on elementary fiber properties is negligible for this class of fibers; however, the theoretical investigations performed up to now[6,7] have primarily focused on establishing the shape and transmission windows of the guided modes and have not, except in the case of circular Bragg fibers,[3] provided a detailed modeling of key quantities such as group-velocity dispersion (GVD), nonlinear coefficients, etc. The purpose of the present work is to model two instances of a simple and well-established design of air-guiding PBG fibers with particular emphasis on the interaction between light and base material, which is here assumed to be silica. Specifically, we derive the fraction of the field energy present in the silica regions of the fiber, the nonlinearity coefficient (expressed as an effective area) arising from the material nonlinearity of silica, and the GVD, including material dispersion effects. We demonstrate that the fraction of the field energy present in the silica is below 10% for both structures studied, and that the nonlinearity coefficients arising from silica are 1–2 orders of magnitude lower than those obtained in the best silica-based, large-mode-area fibers. Furthermore, it will be shown that the GVD is considerably influenced by the dispersion of the base material, and we will demonstrate the reason for this interesting effect by a detailed analysis of the material contributions to the GVD.

The rest of the paper is organized as follows: In Section 2 we describe the fiber designs to be investigated and briefly outline the theoretical approach adopted here, including the basic formulas for group velocity and nonlinearity coefficients. In Section 3 our numerical results are presented and discussed, while Section 4 summarizes our conclusions.

## 2. THEORETICAL APPROACH

The two fiber structures to be investigated are both based on a cladding structure consisting of a triangular lattice of airholes with a core defined by a larger airhole. The structure is characterized by three parameters: the distance between cladding hole centers $\Lambda$, which is commonly denoted the pitch, and the diameters of core and cladding holes. We fix the core hole diameter at $3d$, where $d$ is the cladding hole diameter, and investigate two designs with $d/\Lambda = 0.88$ and $d/\Lambda = 0.95$. A design similar to the former has been modeled earlier by Broeng and co-workers,[6] whereas the latter resembles a low-loss,

 

air-guiding fiber recently fabricated by Venkataraman and co-workers.[5] A schematic picture of the core and nearest cladding region in the design with $d/\Lambda = 0.88$ is shown in Fig. 1.

In the present work we solve Maxwell's equations by expanding the dielectric function and magnetic field vector in plane waves using a freely available software package.[8] Once we obtain the magnetic field vector, the electric fields are calculated straight forwardly by use of Ampere's law. The adoption of a plane-wave basis necessitates the use of periodic boundary conditions; however, the interaction between nearest-neighbor repeated images of the guiding defect can be minimized by a proper choice of the transverse Bloch wave vector.[9] We use a supercell consisting of $8 \times 8$ elementary cells of the triangular lattice comprising the cladding. The Fourier grid used for the plane-wave expansion has $64 \times 64$ mesh points in each elementary cell for the structure with $d/\Lambda = 0.88$, and $96 \times 96$ mesh points for the structure with $d/\Lambda = 0.95$. With these parameters, the dispersion coefficients and all other results are converged within a few percent.

The nonlinear coefficient of a fiber expresses the change in effective index of the guided mode arising from nonlinear effects for a given input power. The dependency of the nonlinear coefficient on the form of the guided mode is usually expressed by an effective area[10]

$$\Delta n_{\text{eff}} = P \frac{n_2^P}{A_{\text{eff}}}. \tag{1}$$

Here $P$ is the power launched into the fiber, and $n_2^P$ is a material nonlinear coefficient (related to the third-order nonlinear susceptibility) in units of $\text{W/m}^2$. For conventional, all-silica fibers, $A_{\text{eff}}$ may be expressed as[10]

$$A_{\text{eff}} = \frac{\left(\int |\mathbf{E}|^2 dA\right)^2}{\int |\mathbf{E}|^4 dA}. \tag{2}$$

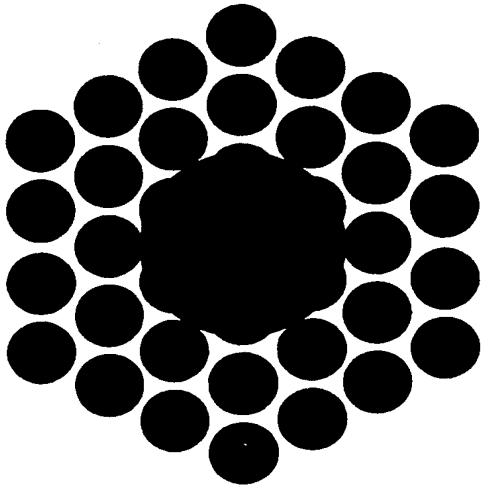

Fig. 1. Schematic picture of one of the structures (with $d/\Lambda = 0.88$) under study. The black circles are airholes while the white areas are the silica regions. Only the core and innermost cladding region are shown.

We have recently shown that for situations in which a substantial part of the field propagates in air, the above definition must be generalized to[11]

$$A_{\text{eff}} = \left(\frac{n_1}{n_g^0}\right)^2 \frac{\left(\int \mathbf{E}\cdot\mathbf{D} dA\right)^2}{\int_{\text{SiO}_2} |\mathbf{E}\cdot\mathbf{D}|^2 dA}. \tag{3}$$

Note that the integration in the denominator is now restricted to the silica parts of the fiber. This formula has been derived without making assumptions about the field energy distribution and is therefore applicable even in the extreme case of air-guiding PBG fibers. Of course, the $A_{\text{eff}}$ values obtained for these fibers have little to do with the physical extent of the guided modes; however, the expression of the nonlinear coefficient in this form facilitates the comparison with more conventional fibers that guide light in silica or other materials.

The GVD coefficient $D$ is defined as

$$D = -\frac{\omega^2}{2\pi c}\frac{d^2\beta}{d\omega^2} = \frac{\omega^2}{2\pi c v_g^2}\frac{dv_g}{d\omega}, \tag{4}$$

where $v_g$ is the group velocity:

$$v_g = \frac{d\omega}{d\beta}. \tag{5}$$

In the present case in which the dielectric function is piecewise constant, the group velocity in the presence of material dispersion effects may be written[9]

$$v_g = \frac{v_g^0}{1 + \frac{\omega}{2} E_d \frac{d\ln\epsilon}{d\omega}}, \tag{6}$$

where $E_d$ is the fraction of the electric field energy present in the dielectric and $v_g^0$ is the group velocity in the absence of material dispersion. The latter may be calculated directly from the fields as[12]

$$v_g^0 = c\frac{\text{Re}\langle[\mathbf{E}^* \times \mathbf{H}]_z\rangle}{\langle \mathbf{H}, \mathbf{H}\rangle}. \tag{7}$$

Thus, the group velocity $v_g$ can be evaluated directly from the fields once the guided mode has been obtained, and the dispersion coefficient can then be calculated by a numerical first-order derivative. This procedure requires that $\omega$, $E_d$, and $v_g^0$ be evaluated at the silica refractive index appropriate for $\omega$, which in the present work is achieved by a self-consistency procedure.[13] The self-consistent calculations are compared with calculations that assume a fixed value of the silica refractive index $n$ to assess the importance of material dispersion effects. In the self-consistent calculations we use the Sellmeier formula for the frequency dependence of the silica refractive index with the coefficients reported by Okamoto.[14]

## 3. NUMERICAL RESULTS

In this work we focus on the guidance of the fundamental mode (whose major transverse part is circularly symmet-

ric) in the lowest bandgap. Initially, we will consider the case of a fixed silica refractive index $n = 1.45$. For this value of $n$, the fiber with $d/\Lambda = 0.88$ is found to have a narrow transmission window for the fundamental mode between $\lambda/\Lambda = 0.724$ and $\lambda/\Lambda = 0.685$, whereas the fiber with $d/\Lambda = 0.95$ has a somewhat wider transmission window between $\lambda/\Lambda = 0.617$ and $\lambda/\Lambda = 0.533$. As will become clear later these transmission windows show some dependence on the material refractive index, which translates into a dependence on the physical value of the pitch (since this controls the physical wavelength of the light in the guided mode). In both fiber designs higher-order modes are present in part of the transmission range of the fundamental mode. For $d/\Lambda = 0.88$ we find that second-order modes are present in the fundamental bandgap in the lower 3/4 of the transmission window for the fundamental mode. For $d/\Lambda = 0.95$ the second-order modes leave the bandgap somewhat earlier, when the fundamental mode is roughly in the middle of the bandgap. Since the question of determining the single-mode wavelength regions of the fibers is complicated by the possibility of guidance in the higher-order bandgaps and is not a primary concern in this paper, we have not attempted a precise determination of the transmission windows for the second-order modes.

In Fig. 2(a) the fraction of the electric field energy present in the silica part of the fibers [$E_d$ in Eq. (6)] is plotted as a function of the distance between the frequency of the fundamental mode and the lower bandgap edge normalized to the gap width. Both fiber designs show the same qualitative behavior: $E_d$ rises as the mode enters or leaves the gap, and therefore a minimum is present inside the transmission window. However, for the design with $d/\Lambda = 0.88$ the minimum is present in the low-frequency part of the transmission window, whereas for $d/\Lambda = 0.95$ the minimum is shifted close to the high-frequency transmission edge. It is also noteworthy that the frequency derivative of $E_d$ is quite large, since the transmission windows are narrow. This has important consequences for the dispersion properties of the fibers.

In Fig. 2(b) the effective areas as calculated from Eq. (3) are plotted for the two fiber designs. The results for $d/\Lambda = 0.88$ have been multiplied by a factor of 10 to facilitate comparison. As expected, very large $A_{\text{eff}}$ values are found, signifying very low nonlinear coefficients. In index-guiding microstructured fibers in the large-mode-area regime ($\lambda \ll \Lambda$), the effective area $A_{\text{eff}} \sim \alpha(d/\Lambda)^{-1}\Lambda^2$ with a numerical prefactor $\alpha$ of the order of 0.5.[15] The fibers are typically operated close to the endlessly-single-mode limit ($d/\Lambda \sim 0.45$), so that $A_{\text{eff}} \sim \Lambda^2$. Typical values of $\Lambda$ are 10–20 $\mu$m, so that $A_{\text{eff}} \sim 100\lambda^2$ for $\lambda \sim 1$ $\mu$m. Thus, the present results for air-guiding PBG fibers indicate a lowering by 1–2 orders of magnitude of the nonlinear coefficient compared with typical index-guiding, large-mode-area microstructured fibers available. Still, it is interesting to observe the significant variation of $A_{\text{eff}}$ over the transmission window and the strong dependence on cladding design of the nonlinear coefficients. In the fiber with $d/\Lambda = 0.88$ a decrease of the effective area with increasing frequency is seen, corresponding to the increasing fraction of field energy in silica [see Eq. (3)]. For $d/\Lambda = 0.95$ the opposite trend occurs because of the shift of the minimum in $E_d$. Of course, the effective areas reported here relate to the nonlinearity coefficients and have little to do with the physical size of the modes. This is better estimated from the standard definition of effective area, Eq. (2), which for both fiber designs is found to be comparable to the area of the hollow core, indicating that the guided mode is well localized.

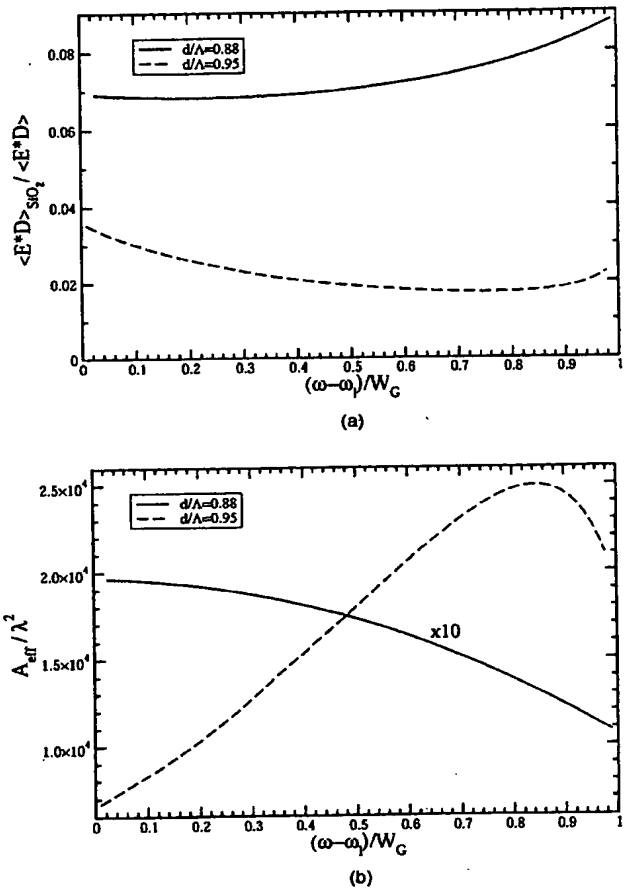


Fig. 2. (a) Field energy fraction in silica, and (b) effective area as calculated from Eq. (3). The effective area curve for the fiber with $d/\Lambda = 0.88$ [solid curve in (b)] has been multiplied by 10 to facilitate comparison.

In Fig. 3 GVD results for three different fiber designs are reported. For the fiber with $d/\Lambda = 0.88$ we have investigated two values of the pitch, $\Lambda = 0.8$ $\mu$m and $\Lambda = 2.4$ $\mu$m. For the design with $d/\Lambda = 0.95$ we show results for $\Lambda = 1.0$ $\mu$m. Both the results of self-consistent calculations and of calculations with a fixed value of the silica dielectric constant are shown. It can be seen that a change in the silica refractive index $n$ shifts the transmission windows and thereby the dispersion curves. Because of the steepness of the dispersion curves, this implies that the dispersion at a given wavelength is strongly dependent on $n$. Therefore, the waveguide GVD calculated at $n = 1.45$ (the solid curves), which is the refractive index of silica at a wavelength of 1.05 $\mu$m, gives a poor prediction of the true chromatic dis-

persion (as given by the self-consistent calculations and reported by the dotted curves) at other wavelengths. The agreement is considerably improved by choosing a fixed index suitable for the wavelength of the guided mode. The results of such calculations are reported by the dashed curves. However, there is still a noticeable difference between the dispersion curves calculated at a fixed $n$ and the self-consistent results. The differences are of the same order of magnitude as the material dispersion of homogeneous silica at the wavelengths in question and are seen to change sign over the transmission window. In Fig. 3(a) it is interesting to note that the dashed and dotted curves do not tend toward each other at the shortest wavelengths of guidance even though the value of $n = 1.46$ used for calculation of the dashed curve corresponds to a wavelength of ~550 nm for pure silica. Instead, the curves cross at a somewhat longer wavelength. These findings indicate that material dispersion effects play a significant role despite the small percentage of field energy present in silica.

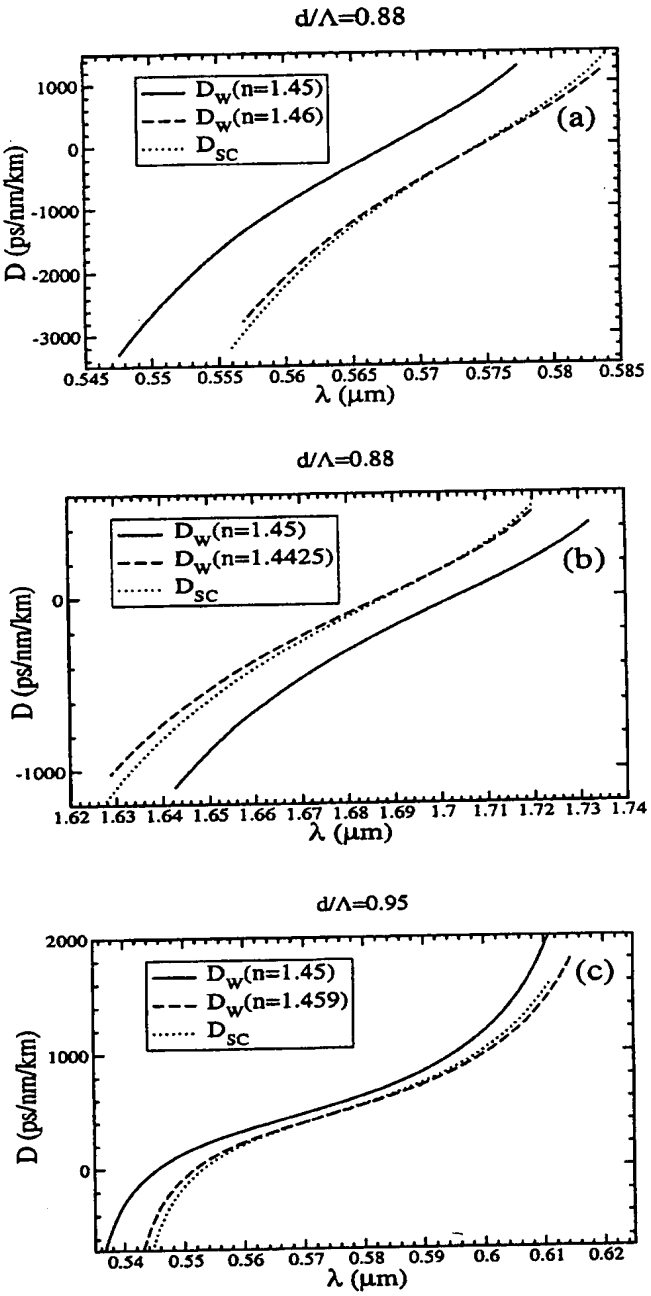


Fig. 3. Dispersion curves for the fundamental guided mode of three air-guiding PBG fibers with various values of $d$ and $\Lambda$: (a) $d/\Lambda = 0.88$, $\Lambda = 0.8\,\mu$m, (b) $d/\Lambda = 0.88$, $\Lambda = 2.4\,\mu$m, (c) $d/\Lambda = 0.95$, $\Lambda = 1.0\,\mu$m. Solid curves report waveguide dispersion ($D_W$) calculated at $n = 1.45$, dashed curves report waveguide dispersion at values of $n$ suitable for the wavelength interval spanned by the transmission window, and dotted curves denote results of self-consistent calculations.

To obtain a more detailed understanding of the influence of material dispersion, we return to Eqs. (4) and (6). The derivative of the group velocity with respect to frequency may be written

$$\frac{dv_g}{d\omega} = \frac{v_g}{v_g^0}\left\{\frac{1}{v_g^0}\frac{\partial v_g^0}{\partial\beta} + \frac{\partial v_g^0}{\partial\epsilon}\frac{d\epsilon}{d\omega} - v_g\left[\frac{E_d}{2}\frac{d\ln\epsilon}{d\omega} + \frac{\omega}{2}\left(\frac{dE_d}{d\omega}\frac{d\ln\epsilon}{d\omega} + E_d\frac{d^2\ln\epsilon}{d\omega^2}\right)\right]\right\}. \quad (8)$$

We adopt a notation where $\partial/\partial\omega$ ($\partial/\partial\beta$) denotes a derivative with respect to $\omega$ ($\beta$) for a fixed value of $\epsilon$, whereas $d/d\omega$ ($d/d\beta$) denotes a derivative including the variation of $\epsilon$ with $\omega$ (and thereby $\beta$). If dispersion in the base material of the fiber is neglected only the first term in Eq. (8) contributes. Using the equation[9]

$$\frac{\partial v_g^0}{\partial\epsilon} = -\frac{E_d}{2\epsilon}v_g^0 - \frac{\omega}{2\epsilon}\frac{\partial E_d}{\partial\beta}, \quad (9)$$

and approximating $dE_d/d\omega \approx \partial E_d/\partial\omega$, which we have found to be reasonably well justified even for the air-guiding fibers studied here, we can write

$$\frac{dv_g}{d\omega} = \frac{v_g}{(v_g^0)^2}\frac{\partial v_g^0}{\partial\beta} - \frac{(v_g)^2}{v_g^0}E_d\left[\frac{d\ln\epsilon}{d\omega}\left(1 + \frac{\omega}{4}E_d\frac{d\ln\epsilon}{d\omega}\right) + \frac{\omega}{2}\frac{d^2\ln\epsilon}{d\omega^2}\right] - \frac{(v_g)^2}{v_g^0}\omega\frac{\partial E_d}{\partial\omega}\frac{d\ln\epsilon}{d\omega}\left(1 + \frac{\omega}{4}E_d\frac{d\ln\epsilon}{d\omega}\right). \quad (10)$$

Thus the GVD may be separated into a part independent of material dispersion effects [first term in Eq. (10)], a part proportional to $E_d$, and a part proportional to the frequency derivative of $E_d$. Using Eq. (4) the GVD is found to be

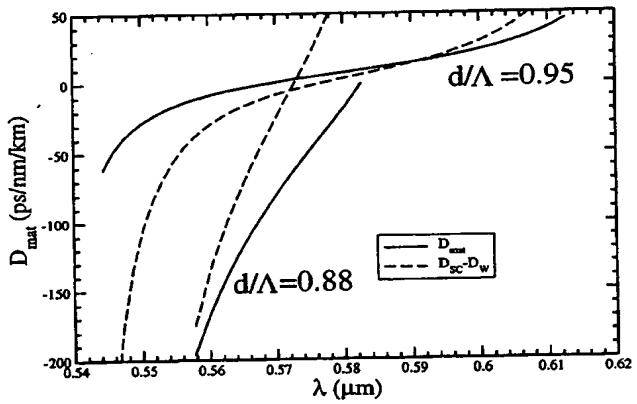


Fig. 4. Material dispersion $D_{\mathrm{mat}}$ (solid curves), defined in Eq. (11), for the two fiber designs guiding at short wavelengths. The dashed curves report the difference between the dotted and dashed curves in Fig. 3 for comparison.

$$D = D_w^{\mathrm{SC}} - \frac{\omega^2 E_d}{2\pi c v_g^0}\left(\frac{\mathrm{d}\ln\epsilon}{\mathrm{d}\omega}\left(1 + \frac{\omega}{4}E_d\frac{\mathrm{d}\ln\epsilon}{\mathrm{d}\omega}\right) + \frac{\omega}{2}\frac{\mathrm{d}^2\ln\epsilon}{\mathrm{d}\omega^2}\right) - \frac{\omega^3}{2\pi c v_g^0}\frac{\partial E_d}{\partial\omega}\frac{\mathrm{d}\ln\epsilon}{\mathrm{d}\omega} \times \left(1 + \frac{\omega}{4}E_d\frac{\mathrm{d}\ln\epsilon}{\mathrm{d}\omega}\right) \equiv D_w^{\mathrm{SC}} + D_{\mathrm{mat}}, \qquad (11)$$

where $D_w^{\mathrm{SC}}$ is the GVD in the absence of material dispersion, but evaluated at the silica refractive index appropriate for the $\omega$ value in question. In Fig. 4 the material dispersion $D_{\mathrm{mat}}$ defined by Eq. (11) is plotted for the two designs guiding at short wavelengths. For the design with $d/\Lambda = 0.88$, where 7–9% of the field energy is in silica, the material dispersion ranges between ~0 and −200 ps/nm/km, whereas for the design with $d/\Lambda = 0.95$ and only 2–3% of the field energy in silica, the material contribution to the GVD ranges between −50 and 50 ps/nm/km. Also shown in Fig. 4 is the difference between the waveguide dispersion at fixed, suitably chosen $n$ (dashed curves in Fig. 3) and the self-consistent dispersion coefficients (dotted curves in Fig. 3). Exact correspondence between solid and dashed curves in Fig. 4 is not to be expected since the waveguide dispersion $D_w^{\mathrm{SC}}$ in Eq. (11) is evaluated at the self-consistent value of $n$; however, it can be seen that the major part of the discrepancy between $D_W$ and $D_{\mathrm{SC}}$ in Fig. 3 can be attributed to the intrinsic material dispersion as expressed by $D_{\mathrm{mat}}$. Since the material dispersion of homogeneous silica in this wavelength range is between −250 and −400 ps/nm/km, the $D_{\mathrm{mat}}$ values reported in Fig. 4 are surprisingly large considering the small values of $E_d$.

It is evident from Eq. (11) that the contribution of material effects to the total GVD of a fiber is composed of a part proportional to $E_d$ and a part proportional to $\partial E_d/\partial\omega$. Herein lies the origin of the surprisingly large $D_{\mathrm{mat}}$ values for the air-guiding fibers: Although $E_d$ is small in these fibers, as is evident from Fig. 2(a), this is not the case for $\partial E_d/\partial\omega$. In Fig. 5 we plot the ratio $R_D$ between the third and second term in Eq. (11):

$$R_D = \frac{\omega\dfrac{\partial\ln E_d}{\partial\omega}\dfrac{\mathrm{d}\ln\epsilon}{\mathrm{d}\omega}}{\dfrac{\mathrm{d}\ln\epsilon}{\mathrm{d}\omega} + \dfrac{\dfrac{\omega}{2}\dfrac{\mathrm{d}^2\ln\epsilon}{\mathrm{d}\omega^2}}{1 + \dfrac{\omega}{4}E_d\dfrac{\mathrm{d}\ln\epsilon}{\mathrm{d}\omega}}}. \qquad (12)$$

The results for the air-guiding fibers in Fig. 5(a) are compared to the results for index-guiding microstructured fibers reported in Fig. 5(b). The latter have a triangular cladding structure similar to the air-guiding fibers, but with a solid silica core defined by a missing airhole. It can be seen that $|R_D|$ for the index-guiding fibers is everywhere below unity, even in the rather extreme case of $d/\Lambda = 0.8$, $\Lambda = 0.34\ \mu$m, where ~15% of the field energy is located in the airholes. For the air-guiding PBG fibers, $|R_D|$ is 1–2 orders of magnitude larger. Thus, for index-guiding microstructured fibers the main contribution to material dispersion effects comes from the second term in Eq. (11), whereas for air-guiding PBG fibers the contribution from the third term dominates.

Because air-guiding PBG fibers have the major part of the field energy propagating in air, the choice of base material is less limited by requirements of low loss and/or nonlinearity than is the case for standard fibers or index-guiding microstructured fibers. On the other hand, the results presented in this work show that the dispersion

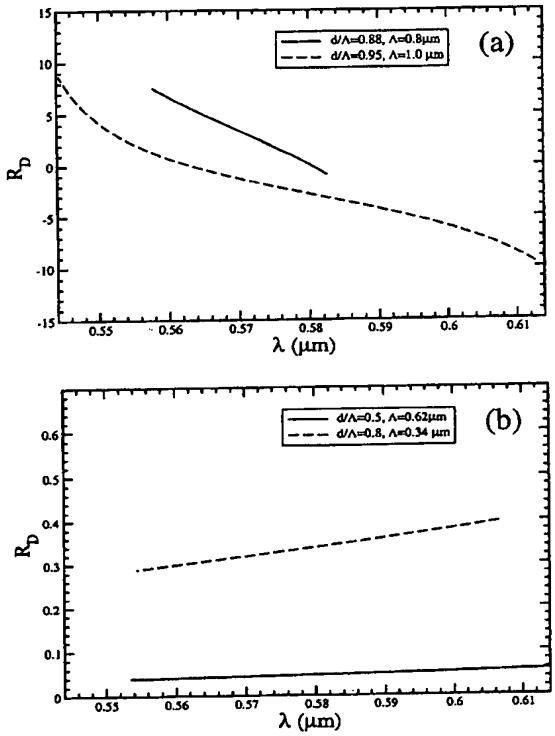


Fig. 5. Plots of the quantity $R_D$, defined in Eq. (12), for two air-guiding PBG fiber designs (a) and two index-guiding fibers (b) having a cladding structure similar (although with smaller airholes) to the air-guiding PBG fibers.

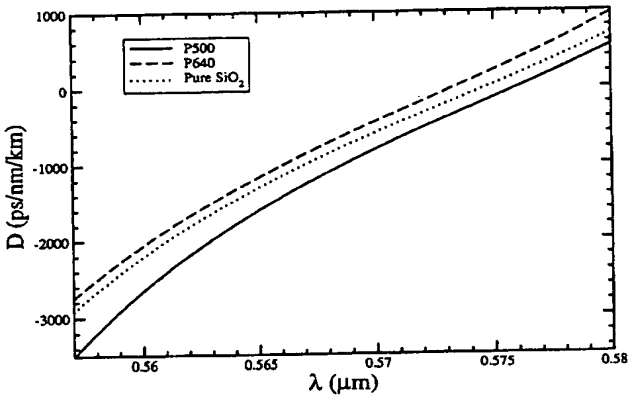


Fig. 6. Dispersion curves for two fibers with added absorption resonances in the base material at either $\lambda = 500$ nm (P500) or $\lambda = 640$ nm (P640) compared to the undoped result.

properties of the material may still have a significant impact on the total GVD of the fiber. These observations suggest that dispersion engineering through the choice of base material may be a possibility in these fibers. A simple example of the possibilities is shown in Fig. 6: The usual three-term Sellmeier polynomial describing the material dispersion of silica has been modified by a fourth term describing the addition of an (dopant) absorption line close to the transmission window of the fiber. The modified Sellmeier polynomial reads:

$$\epsilon(\lambda) = 1 + \sum_{i=1}^{4} \frac{a_i}{\lambda^2 - {\lambda_i}^2}, \tag{13}$$

where

$$a_1 = 0.6965325\ \mu\text{m}^{-2}, \quad \lambda_1 = 0.066\ \mu\text{m};$$

$$a_2 = 0.4083099\ \mu\text{m}^{-2}, \quad \lambda_2 = 0.118\ \mu\text{m};$$

$$a_3 = 0.8968766\ \mu\text{m}^{-2}, \quad \lambda_3 = 9.896\ \mu\text{m};$$

$$a_4 = 0.001\ \mu\text{m}^{-2},$$

with $\lambda_4$ chosen as either 0.5 $\mu$m (P500 in Fig. 6) or 0.640 $\mu$m (P640 in Fig. 6). It is evident that significant shifts of the dispersion curve can be obtained simply by addition of (impurity) absorption centers to the silica matrix. A more general approach would, of course, be to vary the composition of the base material itself as could readily be done in, for example, polymer fibers. Such dispersion engineering could, for instance, be of interest for fibers applied to the kind of gas-phase nonlinearity experiments whose feasibility was recently demonstrated by Benabid and co-workers.[4]

## 4. CONCLUSIONS

In conclusion, we have investigated various aspects of the interplay between the base material and the fundamental guided mode in silica-based, air-guiding PBG fibers. For the two designs studied here, between 2 and 9% of the electric field energy was found to reside in the silica parts of the fiber. The nonlinearity coefficient was expressed in terms of a generalized effective area, which was found to be 1–2 orders of magnitude larger than what can be obtained in index-guiding microstructured fibers. The influence of material dispersion on the total GVD of the fibers was investigated and was found to be of the same order of magnitude as in other fiber types having most of the field energy residing in silica. This effect was traced to the fact that the variation with frequency of the field energy in silica is much more rapid in air-guiding PBG fibers than in other fiber types. These results suggest that dispersion engineering through the choice of base material may be an interesting possibility in air-guiding PBG fibers.

Corresponding author J. Lægsgaard may be reached by e-mail to jl@com.dtu.dk.

## REFERENCES

1. R. F. Cregan, B. J. Mangan, J. C. Knight, T. A. Birks, P. St. J. Russell, P. J. Roberts, and D. C. Allan, "Single-mode photonic band gap guidance of light in air," Science **285**, 1537–1539 (1999).
2. F. Benabid, J. C. Knight, and P. St. J. Russell, "Particle levitation and guidance in hollow-core photonic crystal fiber," Opt. Express **10**, 1195–1203 (2002).
3. G. Ouyang, Y. Xu, and A. Yariv, "Theoretical study on dispersion compensation in air-core Bragg fibers," Opt. Express **10**, 899–908 (2002).
4. F. Benabid, J. C. Knight, G. Antonopoulos, and P. St. J. Russell, "Stimulated Raman scattering in hydrogen-filled hollow-core photonic crystal fiber," Science **298**, 399–402 (2003).
5. N. Venkataraman, M. T. Gallagher, C. M. Smith, D. Müller, J. A. West, K. W. Koch, and J. C. Fajardo, "Low loss (13 db/km) air core photonic bandgap fiber," *28th European Conference on Optical Communication, ECOC '02* (Technical University of Denmark, Kongens Lyngby, Denmark, 2002), post-deadline paper PD1.1.
6. J. Broeng, S. E. Barkou, T. Søndergaard, and A. Bjarklev, "Analysis of air-guiding photonic bandgap fibers," Opt. Lett. **25**, 96–98 (2000).
7. T. P. White, R. C. McPhedran, L. C. Botten, G. H. Smith, and C. Martijn de Sterke, "Calculations of air-guided modes in photonic crystal fibers using the multipole method," Opt. Express **9**, 721–732 (2001).
8. S. G. Johnson and J. D. Joannopoulos, "Block-iterative frequency-domain methods for Maxwell's equations in a planewave basis," Opt. Express **8**, 173–190 (2001).
9. J. Lægsgaard, A. Bjarklev, and S. E. Barkou Libori, "Chromatic dispersion in photonic crystal fibers: fast and accurate scheme for calculation," J. Opt. Soc. Am. B **20**, 1–6 (2003).
10. G. P. Agrawal, *Nonlinear Fiber Optics* (Academic, San Diego, Calif., 2001).
11. J. Lægsgaard, N. A. Mortensen, and A. Bjarklev, "Mode areas and field energy distribution in honeycomb photonic bandgap fibers," J. Opt. Soc. Am. B **20**, 2037–2045 (2003).
12. A. W. Snyder and J. D. Love, *Optical Waveguide Theory* (Chapman & Hall, London, 1996).
13. S. E. Barkou, J. Broeng, and A. Bjarklev, "Dispersion properties of photonic bandgap guiding fibers," in *Optical Fiber Communication Conference*, (OFC) (1999) (Optical Society of America, Washington, D.C., 1999), pp. 117–119.
14. K. Okamoto, *Fundamentals of Optical Waveguides* (Academic, San Diego, Calif., 2000).
15. N. A. Mortensen, "Effective area of photonic crystal fibers," Opt. Express **10**, 341–348 (2002).

# Silica-glass contribution to the effective nonlinearity of hollow-core photonic band-gap fibers

**Christopher J. Hensley, Dimitre G. Ouzounov and Alexander L. Gaeta**
*School of Applied & Engineering Physics, Cornell University, Ithaca, NY 14853*
cjh55@cornell.edu, alg3@cornell.edu

**Natesan Venkataraman, Michael T. Gallagher and Karl W. Koch**
*Corning Inc, Corning, NY 14831*

**Abstract:** We measure the effective nonlinearity of various hollow-core photonic band-gap fibers. Our findings indicate that differences of tens of nanometers in the fiber structure result in significant changes to the power propagating in the silica glass and thus in the effective nonlinearity of the fiber. These results show that it is possible to engineer the nonlinear response of these fibers via small changes to the glass structure.



**OCIS codes:** (060.2319) Fiber optics; (060.4370) Nonlinear optics, fibers;

## References and links

1. R. F. Cregan, B. J. Mangan, J. C. Knight, T. A. Birks, P. St. J. Russell, P. J. Roberts, and D. A. Allan, "Single-mode photonic band gap guidnce of light in air," Science **285**, 1537-1539 (1999).
2. D. C. Allan, J. A. West, J. C. Fajardo, M. T. Gallagher, K. W. Koch, and N. F. Borrelli, "Photonic crystal fibers: effective-index and band-gap guidance," in *Photonic crystals and Light Localization in the 21st Century*, C. M. Soukoulis, ed. (Kluwer Academic, Dordecht, Netherlands, 2001) pp. 305-320.
3. J. A. West, N. Venkataraman, C. M. Smith, and M. T. Gallagher, "Photonic Crystal Fibers" in *Proceedings of European Conference on Optical Communication* (IEEE, 2001) pp. 582-585.
4. C. M. Smith, N. Venkataraman, M. T. Gallagher, D. Muller, J. A. West, N. F. Borrelli, D. C. Allan, and K. W. Koch, "Low-loss hollow-core silica/air photonic bandgap fibre," Nature **424**, 657-659 (2003).
5. P. Roberts, F. Couny, H. Sabert, B. Mangan, D. Williams, L. Farr, M. Mason, A. Tomlinson, T. Birks, J. Knight, and P. St. J. Russell, "Ultimate low loss of hollow-core photonic crystal fibres," Opt. Express **13**, 236-244 (2005), http://www.opticsexpress.org/abstract.cfm?URI=OPEX-13-1-236.
6. D. G. Ouzounov, F. R. Ahmad, D. Muller, N. Venkataraman, M. T. Gallagher, M. G. Thomas, J. Silcox, K. W. Koch, and A. L. Gaeta, "Generation of megawatt optical solitons in hollow-core photonic band-gap fibers," Science **301**, 1702-1704 (2003).
7. F. Luan, J. C. Knight, P. St. J. Russell, S. Campbell, D. Xiao, D. T. Reid, B. J. Mangan, D. P. Williams and P. J. Roberts, "Femtosecond soliton pulse delivery at 800 nm wavelength in hollow-core photonic bandgap fibers," Opt. Express **12**, 835-840 (2004), http://www.opticsexpress.org/abstract.cfm?URI=OPEX-12-5-835.
8. G. Humbert, J. C. Knight, G. Bouwmans, P. St. J. Russell, D. P. Williams, P. J. Roberts, B. J. Mangan, "Hollow core photonic crystal fibers for beam delivery," Opt. Express **12**, 1477-1484 (2004), http://www.opticsexpress.org/abstract.cfm?URI=OPEX-12-8-1477.

#77836 - $15.00 USD
Received 7 December 2006; revised 9 February 2007; accepted 9 February 2007

9. J. D. Shephard, J. D. C. Jones, D. P. Hand, G. Bouwmans, J. C. Knight, P. St. J. Russell, and B. J. Mangan, "High energy nanosecond laser pulses delivered single-mode through hollow-core PBG fibers," Opt. Express **12**, 717-723 (2004), http://www.opticsexpress.org/abstract.cfm?URI=OPEX-12-4-717.
10. J. Limpert, T. Schreiber, S. Nolte, H. Zellmer and A. Tünnermann, "All fiber chirped-pulse amplification system based on compression in air-guiding photonic bandgap fiber," Opt. Express **11**, 3332-3337 (2003), http://www.opticsexpress.org/abstract.cfm?URI=OPEX-11-24-3332.
11. H. Lim and F. W. Wise, "Control of dispersion in a femtosecond ytterbium laser by use of hollow-core photonic bandgap fiber," Opt. Express **12**, 2231-2235 (2004), http://www.opticsexpress.org/abstract.cfm?URI=OPEX-12-10-2231.
12. C. de Matos, J. Taylor, T. Hansen, K. Hansen, and J. Broeng, "All-fiber chirped pulse amplification using highly-dispersive air-core photonic bandgap fiber," Opt. Express **11**, 2832-2837 (2003), http://www.opticsexpress.org/abstract.cfm?URI=OPEX-11-22-2832.
13. M. Rusu and O. G. Okhotnikov, "All-fiber picosecond laser source based on nonlinear spectral compression," Appl. Phys. Lett. **89**, 091118 (2006).
14. C. K. Nielsen, K. G. Jespersen, and S. R. Keiding, "A 158 fs 5.3 nJ fiber-laser system at 1 $\mu$m using photonic bandgap fibers for dispersion control and pulse compression," Opt. Express **14**, 6063-6068 (2006), http://www.opticsinfobase.org/abstract.cfm?URI=OPEX-14-13-6063.
15. J. Lægsgaard, N. A. Mortensen, J. Riishede and A. Bjarklev, "Material effects in air-guiding photonic bandgap fibers," J. Opt. Soc. Am. B **20**, 2046-2051 (2003).
16. I. V. Fedotov, A. B. Fedotov, and A. M. Zheltikov, "Raman-resonance-enhanced composite nonlinearity of air-guided modes in hollow photonic-crystal fibers," Opt. Lett. **31**, 2604-2606 (2006).
17. J. A. West, C. M. Smith, N. F. Borrelli, D. C. Allan and K. W. Koch, "Surface modes in air-core photonic band-gap fibers," Opt. Express **12**, 1485-1496 (2004), http://www.opticsexpress.org/abstract.cfm?URI=OPEX-12-8-1485.
18. P. J. Roberts, D. P. Williams, B. J. Mangan, H. Sabert, F. Couny, W. J. Wadsworth, T. A. Birks, J. C. Knight and P. St. J. Russell, "Realizing low loss air core photonic crystal fibers by exploiting an antiresonant core surround," Opt. Express **13**, 8277-8285 (2005), http://www.opticsexpress.org/abstract.cfm?URI=OPEX-13-20-8277.
19. M. Oberthaler and R. A. Höpfel, "Spectral narrowing of ultrashort laser pulses by self-phase modulation in optical fibers," Appl. Phys. Lett. **63**, 1017-1019 (1993).
20. T. Brabec and F. Krausz, "Nonlinear optical pulse propagation in the single-cycle regime," Phys. Rev. Lett. **78**, 3282-3285 (1997).
21. D. Blömer, A. Szameit, F. Dreisow, T. Schreiber, S. Nolte and A. Tünnermann, "Nonlinear refractive index of fs-laser-written waveguides in fused silica," Opt. Express **14**, 2151-2157 (2006), http://www.opticsexpress.org/abstract.cfm?URI=OPEX-14-6-2151.
22. G. P. Agrawal, *Nonlinear Fiber Optics* (Academic Press, 1989).
23. R. W. Boyd, *Nonlinear Optics* (Academic Press, ed. 2, 2003).

Hollow-core photonic band-gap fibers (HC-PBGF's), which guide light via interference from the two-dimensional microstructure surrounding the air-core, have attracted significant interest since their first demonstration [1]. PBGF's confine light in the low-refractive index of air and offer the potential of lower loss and nonlinearity than standard step-index silica fibers. The complicated, nanometer-scale structure of PBGF's makes fabrication of these fibers challenging, and the attenuation of early samples was approximately 1000 dB/km [2,3]. A significant reduction of loss was achieved with the development of a PBGF with an attenuation of 13 dB/km, which brought the loss to a level where HC-PBGFs could find practical utilization [4]. More recently, a larger-core multimode PBGF was demonstrated with a loss of 1.7 dB/km [5].

To find applications in telecommunications, PBGF's will need to exhibit loss that is comparable to or less than that of step-index silica fibers. However, there are other applications that require delivery of high-energy pulses, for which HC-PBGF's have already demonstrated significant advantages over glass-core fibers [6–9]. A generic feature of HC-PBGF's is that the group-velocity dispersion (GVD) is anomalous over most of the transmission window [6], which makes them suitable for dispersive elements in high-power fiber lasers and amplifiers [10–14]. Low nonlinearity is crucial for preserving the fidelity of propagating pulses, and it is important to understand the contribution from

#77836 - $15.00 USD Received 7 December 2006; revised 9 February 2007; accepted 9 February 2007

both the glass and air regions. The optical field is primarily localized in the air core, but since the nonlinear refractive index of glass is roughly 1000× larger than air, it is not obvious which medium dominates the effective nonlinearity of the fiber. It was shown [6] that the effective nonlinearity of the fundamental mode of the fiber described in Ref. 4 is approximately equal to that of the air in the fiber core. Alternatively, theoretical analysis of commercially available HC-PBGFs [7,8] concluded that glass and air regions have comparable contributions to the total nonlinearity. Lægsgaard *et al.* [15] showed theoretically that the fraction of light that resides in the silica regions, which yields the glass contribution to total nonlinearity, depends strongly on the air-filling fraction—defined by the fractional area that air comprises within a unit cell in the holey cladding region. Recent work [16] using coherent anti-Stokes Raman scattering investigated the nonlinear contribution of glass at transmission edges of the band-gap.

In this paper, we report on an experimental investigation of the silica-glass contribution to the effective nonlinearity of several HC-PBGF's with different air-filling fractions. We find that the silica contribution can vary over a broad range depending on small variations in fiber structure. By confining the mode to the air core, it is possible to reduce nonlinearity and loss [17]. These results are consistent with studies of the structural mechanism for light confinement within the air core [18].

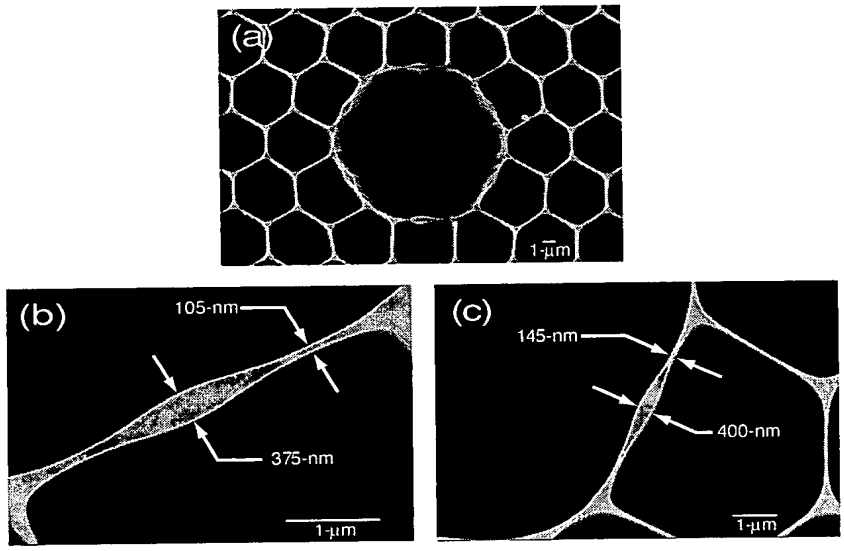


Fig. 1. (a) SEM image of Corning fiber I. All three fibers characterized in this work have this same general structure. Closeup SEM of air-core wall of Corning fiber II (b) and Corning fiber III (c). Indicated dimensions have an error of ±5 nm.

In our experiments, we study three different fibers manufactured by Corning. Two of these fibers, Corning fiber II (CF2) and fiber III (CF3), have operational ranges centered at 1255 nm, while the third, Corning fiber I (CF1) [4], has a zero-GVD wavelength at 1425 nm with the transmission window centered at 1475 nm. Scanning electron microscope (SEM) images of the core walls (Figs. 1(b) and 1(c)) illustrate the tens of nanometers differences within the fiber profiles. The indicated widths are consistent with measurements taken around the core and along the length of the fibers to within the resolution of the SEM images. The air-filling fraction of the CF1 is 0.94, while the

#77836 - $15.00 USD
Received 7 December 2006; revised 9 February 2007; accepted 9 February 2007

values for CF2 and CF3 are 0.95 and 0.96, respectively. However, as we will show, the air-filling fraction is not the sole parameter that determines the fiber nonlinearity.

The experimental setup is shown in Fig. 2. Pulses are produced by a regenerative amplification system (Hurricane, Spectra Physics) seeded by a Ti-sapphire oscillator. This 1-kHz source centered at 800 nm is used to pump an optical parametric amplifier (OPA) that supplies 100-fs pulses tunable from 1100 to 1600 nm. Using an aspheric 10× objective, the beam is coupled into the fiber, which is held inside a vacuum chamber. The coupling efficiency for all these fibers is 50% - 55%. We couple 100-fs pulses at the zero-GVD wavelength (1255 nm for CF2 and CF3 and 1425 nm for CF1) and measure the output pulse spectrum and autocorrelation when the fiber holes are filled with air and when the chamber is evacuated to a pressure less than 30 mTorr.

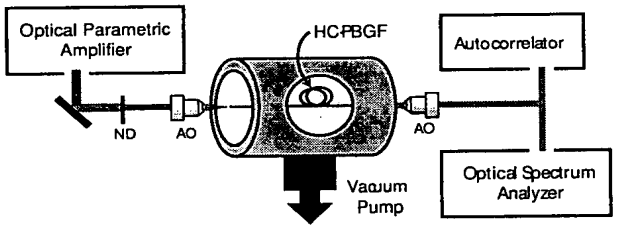


Fig. 2. Experimental setup showing the beam from the femtosecond optical parametric amplifier attenuated by neutral density filters (ND) and then coupled in and out of the hollow-core photonic band-gap fiber (HC-PBGF) by two 10× aspheric objectives (AO).

In an effort to calibrate our results to previously reported data, Fig. 3(a) shows the transmitted pulse spectrum for the commercially available HC-800-01 fiber. For 100-nJ pulses propagating through the air-filled fiber, the spectrum is nearly identical to that of 200-nJ pulses propagating in vacuum, indicating that the silica-glass structure and air have nearly equal contributions to the effective fiber nonlinearity, which is in good agreement with the theoretical results of Ref. 7. The pulses of the regenerative system used in these measurements carry a small negative chirp, which explains the spectral narrowing of the output pulse spectra [19]. Fig. 3(b) shows the output spectrum for 2-$\mu$J pulses propagating through the evacuated core of CF1. The absence of structure or spectral broadening at these high pulse energies indicates that the fiber nonlinearity is dominated by air. It has been shown that 900-nJ, 110-fs pulses in an air-filled core undergo significant soliton self-frequency shifting due to Raman scattering [6].

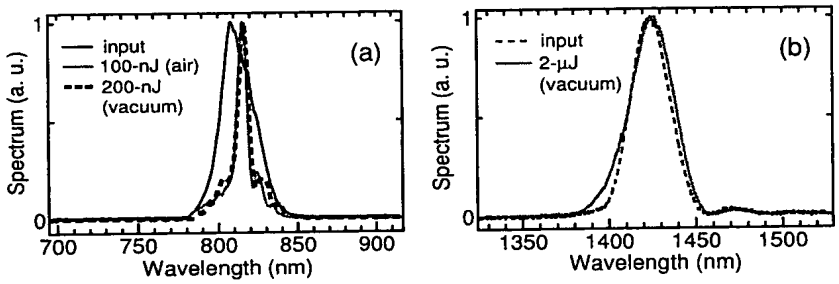


Fig. 3. (a) Output spectra for energies of pulses propagating in air and vacuum in the HC-800-01 fiber that produces nearly identical spectral shapes. (b) Output spectrum for a pulse with an energy of 2 $\mu$J propagating in vacuum for Corning fiber I.

#77836 - $15.00 USD
Received 7 December 2006; revised 9 February 2007; accepted 9 February 2007

To quantify better the glass contribution to the total nonlinearity, we simulated pulse propagation with the generalized nonlinear Schrodinger equation, which includes third- and fourth-order dispersion, and self-steepening [20]. This method has recently been used to investigate nonlinearity in fs-written waveguides [21]. In our simulations we define the relative intensity $\eta$ in silica as the fraction of the peak field intensity $I_{silica}$ in the silica glass to that $I_{core}$ in the hollow-core, that is, $\eta = I_{silica}/I_{core}$.

For an evacuated fiber, we use the nonlinear length definition [22] and solve for the total effective nonlinearity,

$$L_{NL} = \frac{\lambda}{2\pi n_2 I_o^{silica}} = \frac{\lambda}{2\pi n_2 \eta I_o^{core}} = \frac{1}{\gamma_{eff} P_o^{core}}. \quad (1)$$

Here $\gamma_{eff} = \eta 2\pi n_2/\lambda A_{eff}$ is the total effective nonlinearity, $n_2 = 2.6 \times 10^{-16}$ cm$^2$/W is the nonlinear refractive index of silica, $A_{eff}$ is the mode field area ($\sim$70-$\mu$m$^2$ for all these fibers), and $\lambda$ is the wavelength. In our simulations $\eta$ is varied until the best fit of theory to the measured output spectrum is achieved.

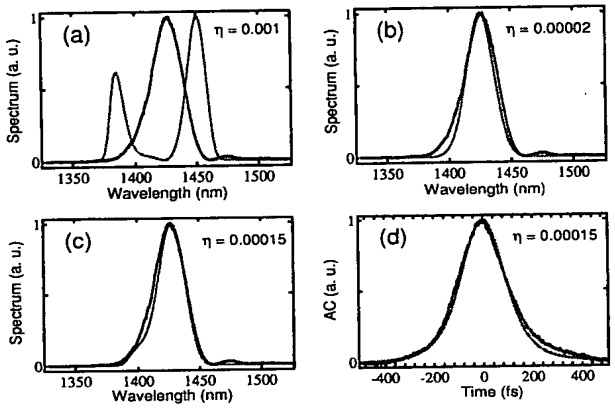


Fig. 4. Several iterations are shown to produce the best numerical fit (red) for the experimental output spectrum (black) for a 2.054-$\mu$J pulse energy in Corning fiber I [(a)-(c)]. In addition, we show the numerical best fit (red) and experimental (black) output autocorrelation (d).

By this method, we find that the relative intensity in silica for CF1 is 0.015% (Fig. 4). To obtain the best agreement, we used a slightly larger value for the third-order dispersion than that reported [6]. Repeating this process of varying $\eta$ in our simulation to fit the measured output spectra for CF2 and CF3 yields relative intensities of 0.10% and 0.042%, respectively. Thus the glass contribution to the effective nonlinearity of CF1 is approximately 7$\times$ smaller than that of CF2 and 3$\times$ smaller than that of CF3. The resulting total effective nonlinearities $\gamma_{eff}$ are summarized below in Table 1, and for comparison we have listed the value for standard step-index fiber (SMF-28). In the final column we have also included the case for the air-filled fiber at 1 atm with $n_2^{air} = 5.0 \times 10^{-19}$ cm$^2$/W [23].

As a final demonstration of this structurally sensitive nonlinearity, we measure the spectral broadening of the output pulse as a function of pulse energy (see Fig. 5). For this experiment, transform-limited pulses are coupled into evacuated fibers at the zero-dispersion wavelength. Under these conditions, changes to the spectral full-width-at-half-maximum are attributed entirely to the nonlinearity of the fiber [22]. These

#77836 - $15.00 USD
Received 7 December 2006; revised 9 February 2007; accepted 9 February 2007

Table 1. Effective fiber nonlinearity $\gamma_{eff}$, for various fibers.

| | $\gamma_{eff}$ ($W^{-1}$/cm) | |
|---|---|---|
| Fiber type | Evacuated core | Air-filled core |
| Corning fiber I | $2.4 \times 10^{-9}$ | $3.4 \times 10^{-8}$ |
| Corning fiber II | $1.9 \times 10^{-8}$ | $5.4 \times 10^{-8}$ |
| Corning fiber III | $7.7 \times 10^{-9}$ | $4.3 \times 10^{-8}$ |
| Step-index fiber | $5 \times 10^{-5}$ | |

results are consistent with our previous data showing that similar broadening occurs at lower peak powers for CF2 due to the greater contribution of silica glass to the total nonlinearity in this fiber (Fig. 5).

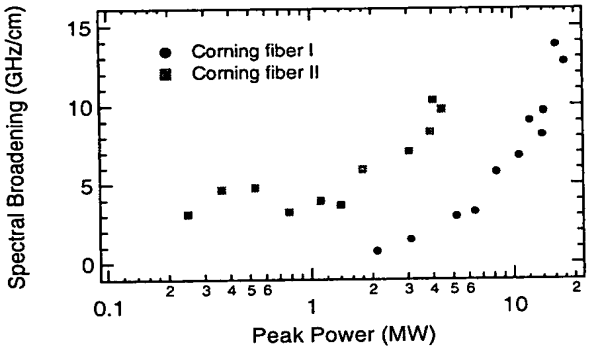


Fig. 5. Output pulse spectral broadening per unit fiber length for Corning fiber I (circles) and fiber II (squares).

In conclusion, we determine experimentally the silica-glass contribution to the effective nonlinearity of three hollow-core photonic band-gap fibers. We find that the relative power in the silica—normalized to that in the air-core region—can vary by nearly an order of magnitude and is highly sensitive to the fiber structure. As a result, the contribution of silica glass to the effective fiber nonlinearity, and thus to the total nonlinearity, can be engineered over broad limits through small structural changes. These results are relevant to applications involving delivery of high-power pulses, where by evacuating the fiber core the majority of the fiber nonlinearity can be eliminated.


## Acknowledgments

This work was supported by the Air Force Office of Scientific Research under contract number F49620-03-1-0223 and by the Center for Nanoscale Systems supported by NSF under award number EEC-0117770. CJH acknowledges financial support from Lawrence Livermore National Laboratories through the NPSC. The LEO 1550 SEM was originally funded by the Keck Foundation, with additional support from the Cornell Nanobiotechnology Center (STC program, NSF award number ECS-9876771).



#77836 - $15.00 USD



Received 7 December 2006; revised 9 February 2007; accepted 9 February 2007

## WILEY SERIES IN MICROWAVE AND OPTICAL ENGINEERING

**KAI CHANG**, Editor
*Texas A&M University*

FIBER-OPTIC COMMUNICATION SYSTEMS, Second Edition • *Govind P. Agrawal*
COHERENT OPTICAL COMMUNICATIONS SYSTEMS • *Silvello Betti, Giancarlo De Marchis and Eugenio Iannone*
HIGH-FREQUENCY ELECTROMAGNETIC TECHNIQUES: RECENT ADVANCES AND APPLICATIONS • *Asoke K. Bhattacharyya*
COMPUTATIONAL METHODS FOR ELECTROMAGNETICS AND MICROWAVES • *Richard C. Booton, Jr.*
MICROWAVE RING CIRCUITS AND ANTENNAS • *Kai Chang*
MICROWAVE SOLID-STATE CIRCUITS AND APPLICATIONS • *Kai Chang*
DIODE LASERS AND PHOTONIC INTEGRATED CIRCUITS • *Larry Coldren and Scott Corzine*
MULTICONDUCTOR TRANSMISSION-LINE STRUCTURES: MODAL ANALYSIS TECHNIQUES • *J. A. Brandão Faria*
PHASED ARRAY-BASED SYSTEMS AND APPLICATIONS • *Nick Fourikis*
FUNDAMENTALS OF MICROWAVE TRANSMISSION LINES • *Jon C. Freeman*
MICROSTRIP CIRCUITS • *Fred Gardiol*
HIGH-SPEED VLSI INTERCONNECTIONS: MODELING, ANALYSIS, AND SIMULATION • *A. K. Goel*
HIGH-FREQUENCY ANALOG INTEGRATED CIRCUIT DESIGN • *Ravender Goyal (ed.)*
FINITE ELEMENT SOFTWARE FOR MICROWAVE ENGINEERING • *Tatsuo Itoh, Giuseppe Pelosi and Peter P. Silvester (eds.)*
OPTICAL COMPUTING: AN INTRODUCTION • *M. A. Karim and A. S. S. Awwal*
MILLIMETER WAVE OPTICAL DIELECTRIC INTEGRATED GUIDES AND CIRCUITS • *Shiban K. Koul*
MICROWAVE DEVICES, CIRCUITS AND THEIR INTERACTION • *Charles A. Lee and G. Conrad Dalman*
ADVANCES IN MICROSTRIP AND PRINTED ANTENNAS • *Kai-Fong Lee and Wei Chen (eds.)*
OPTOELECTRONIC PACKAGING • *A. R. Mickelson, N. R. Basavanhally, and Y. C. Lee (eds.)*
ANTENNAS FOR RADAR AND COMMUNICATIONS: A POLARIMETRIC APPROACH • *Harold Mott*
INTEGRATED ACTIVE ANTENNAS AND SPATIAL POWER COMBINING • *Julio A. Navarro and Kai Chang*
FREQUENCY CONTROL OF SEMICONDUCTOR LASERS • *Motoichi Ohtsu (ed.)*
SOLAR CELLS AND THEIR APPLICATIONS • *Larry D. Partain (ed.)*
ANALYSIS OF MULTICONDUCTOR TRANSMISSION LINES • *Clayton R. Paul*
INTRODUCTION TO ELECTROMAGNETIC COMPATIBILITY • *Clayton R. Paul*
INTRODUCTION TO HIGH-SPEED ELECTRONICS AND OPTOELECTRONICS • *Leonard M. Riaziat*
NEW FRONTIERS IN MEDICAL DEVICE TECHNOLOGY • *Arye Rosen and Harel Rosen (eds.)*
NONLINEAR OPTICS • *E. G. Sauter*
FREQUENCY SELECTIVE SURFACE AND GRID ARRAY • *T. K. Wu (ed.)*
ACTIVE AND QUASI-OPTICAL ARRAYS FOR SOLID-STATE POWER COMBINING • *Robert A. York and Zoya B. Popović (eds.)*
OPTICAL SIGNAL PROCESSING, COMPUTING AND NEURAL NETWORKS • *Francis T. S. Yu and Suganda Jutamulia*

# Fiber-Optic Communication Systems

## Second Edition

**GOVIND P. AGRAWAL**
*The Institute of Optics*
*University of Rochester*
*Rochester, NY*

A WILEY-INTERSCIENCE PUBLICATION
**JOHN WILEY & SONS, INC.**
NEW YORK / CHICHESTER / WEINHEIM / BRISBANE / SINGAPORE / TORONTO

This text is printed on acid-free paper.



*Library of Congress Cataloging in Publication Data:*

Agrawal, G. P. (Govind P.), 1951-
Fiber-optic communication systems / Govind P. Agrawal. — 2nd ed.
p. cm. — (Wiley series in microwave and optical engineering)
"A Wiley-Interscience publication."
Includes index.
ISBN 0-471-17540-4 (cloth : alk. paper)
1. Optical communications. 2. Fiber optics. I. Title.
II. Series.
TK5103.59.A37 1997 97-4040
621.382'75—dc21

Printed in the United States of America

10 9 8 7 6 5 4 3 2

*For My Parents*

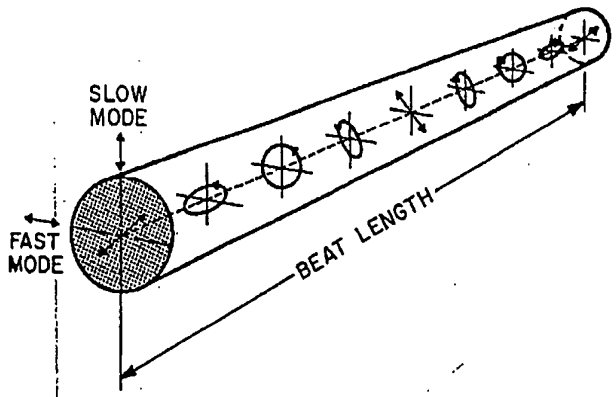


**Figure 2.6** State of polarization in a birefringent fiber over one beat length. Input beam is linearly polarized at 45° with respect to the slow and fast axes.

necessary to employ polarization-insensitive coherent receivers. It is possible to make fibers for which random fluctuations in the core shape and size are not the governing factor in determining the state of polarization. Such fibers are called polarization-preserving fibers. A large amount of birefringence is introduced intentionally in these fibers through design modifications so that small random birefringence fluctuations do not affect the light polarization significantly. Typically, $B \sim 10^{-4}$ for such fibers.

### Spot Size

Since the field distribution given by Eq. (2.2.42) is cumbersome to use in practice, it is often approximated by a *Gaussian distribution* of the form

$$E_x = A \exp(-\rho^2/w^2) \exp(i\beta z), \tag{2.2.45}$$

where $w$ is the *field radius* and is referred to as the *spot size*. It is determined by fitting the exact distribution to the Gaussian function or by following a variational procedure [32]. Figure 2.7 shows the dependence of $w/a$ on the $V$ parameter. A comparison of the actual field distribution with the fitted Gaussian is also shown for $V = 2.4$. The quality of fit is generally quite good for values of $V$ in the neighborhood of 2. The spot size $w$ can be determined from Fig. 2.7. It can also be determined from an analytic approximation accurate to within 1% for $1.2 < V < 2.4$ and given by [32]

$$w/a \approx 0.65 + 1.619V^{-3/2} + 2.879V^{-6}. \tag{2.2.46}$$

The fraction of the power contained in the core can be obtained by using Eq. (2.2.45) and is given by the *confinement factor*

$$\Gamma = \frac{P_{\text{core}}}{P_{\text{total}}} = \frac{\int_0^a |E_x|^2 \rho \, d\rho}{\int_0^\infty |E_x|^2 \rho \, d\rho} = 1 - \exp\left(-\frac{2a^2}{w^2}\right). \tag{2.2.47}$$



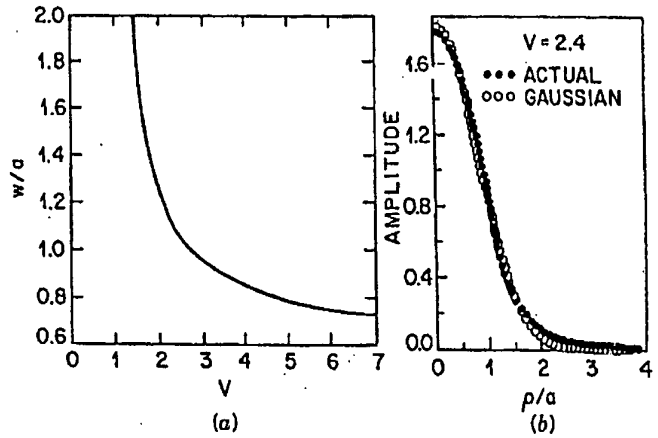


**Figure 2.7** (a) Normalized spot size $w/a$ as a function of the $V$ parameter obtained by fitting the fundamental fiber mode to a Gaussian distribution; (b) quality of fit for $V = 2.4$. (After Ref. [32]. ©1978 OSA. Reprinted with permission.)

Equations (2.2.46) and (2.2.47) determine the fraction of the mode power contained inside the core for a given value of $V$. Although nearly 75% of the mode power resides in the core for $V = 2$, this percentage drops down to 20% for $V = 1$. For this reason most telecommunication single-mode fibers are designed to operate in the range $2 < V < 2.4$.

## 2.3 DISPERSION IN SINGLE-MODE FIBERS

It was seen in Section 2.1 that intermodal dispersion in multimode fibers leads to considerable broadening of short optical pulses ($\sim 10$ ns/km). In the geometrical-optics description, such broadening was attributed to different paths followed by different rays. In the modal description it is related to the different mode indices (or group velocities) associated with different modes. The main advantage of single-mode fibers is that intermodal dispersion is absent simply because the energy of the injected pulse is transported by a single mode. However, pulse broadening does not disappear altogether. The group velocity associated with the fundamental mode is frequency dependent because of chromatic dispersion. As a result, different spectral components of the pulse travel at slightly different group velocities, a phenomenon referred to as *group-velocity dispersion* (GVD), *intramodal dispersion*, or simply *fiber dispersion*. Intramodal dispersion has two contributions, material dispersion and waveguide dispersion. We consider both of them and discuss how GVD limits the performance of lightwave systems employing single-mode fibers.

### 2.3.1 Group-Velocity Dispersion

Consider a single-mode fiber of length $L$. A specific spectral component at the frequency $\omega$ would arrive at the output end of the fiber after a time delay $T = L/v_g$, where $v_g$ is the *group velocity*, defined as [22]

$$v_g = (d\beta/d\omega)^{-1}. \tag{2.3.1}$$

By using $\beta = \bar{n}k_0 = \bar{n}\omega/c$ in Eq. (2.3.1), one can show that $v_g = c/\bar{n}_g$, where $\bar{n}_g$ is the *group index* given by

$$\bar{n}_g = \bar{n} + \omega(d\bar{n}/d\omega). \tag{2.3.2}$$

The frequency dependence of the group velocity leads to pulse broadening simply because different spectral components of the pulse disperse during propagation and do not arrive simultaneously at the fiber output. If $\Delta\omega$ is the spectral width of the pulse, the extent of pulse broadening for a fiber of length $L$ is governed by

$$\Delta T = \frac{dT}{d\omega}\Delta\omega = \frac{d}{d\omega}\left(\frac{L}{v_g}\right)\Delta\omega = L\frac{d^2\beta}{d\omega^2}\Delta\omega = L\beta_2\Delta\omega, \tag{2.3.3}$$

where Eq. (2.3.1) was used. The parameter $\beta_2 = d^2\beta/d\omega^2$ is known as the GVD parameter. It determines how much an optical pulse would broaden on propagation inside the fiber.

In some optical communication systems, the frequency spread $\Delta\omega$ is determined by the range of wavelengths $\Delta\lambda$ emitted by the optical source. It is customary to use $\Delta\lambda$ in place of $\Delta\omega$. By using $\omega = 2\pi c/\lambda$ and $\Delta\omega = (-2\pi c/\lambda^2)\Delta\lambda$, Eq. (2.3.3) can be written as

$$\Delta T = \frac{d}{d\lambda}\left(\frac{L}{v_g}\right)\Delta\omega = DL\Delta\lambda, \tag{2.3.4}$$

where

$$D = \frac{d}{d\lambda}\left(\frac{1}{v_g}\right) = -\frac{2\pi c}{\lambda^2}\beta_2. \tag{2.3.5}$$

$D$ is called the *dispersion parameter* and is expressed in units of ps/(km-nm).

The effect of dispersion on the bit rate $B$ can be estimated by using the criterion $B\Delta T < 1$ in a manner similar to that used in Section 2.1. By using $\Delta T$ from Eq. (2.3.4) this condition becomes

$$BL|D|\Delta\lambda < 1. \tag{2.3.6}$$

Equation (2.3.6) provides an order-of-magnitude estimate of the $BL$ product offered by single-mode fibers. The wavelength dependence of $D$ is studied in the next two subsections. For standard silica fibers, $D$ is relatively small in the wavelength region near 1.3 $\mu$m [$D \sim 1$ ps/(km-nm)]. For a semiconductor laser, the spectral width $\Delta\lambda$ is 2–4 nm even when the laser operates in several longitudinal modes. The $BL$ product of such lightwave systems can exceed



100 (Gb/s)-km. Indeed, 1.3-$\mu$m telecommunication systems typically operate at a bit rate of 2 Gb/s with a repeater spacing of 40–50 km. The $BL$ product of single-mode fibers can exceed 1 (Tb/s)-km when single-mode semiconductor lasers (see Section 3.3) are used to reduce $\Delta\lambda$ below 1 nm.

The dispersion parameter $D$ can vary considerably when the operating wavelength is shifted from 1.3 $\mu$m. The wavelength dependence of $D$ is governed by the frequency dependence of the mode index $\bar{n}$. From Eq. (2.3.5), $D$ can be written as

$$D = -\frac{2\pi c}{\lambda^2}\frac{d}{d\omega}\left(\frac{1}{v_g}\right) = -\frac{2\pi}{\lambda^2}\left(2\frac{d\bar{n}}{d\omega} + \omega\frac{d^2\bar{n}}{d\omega^2}\right), \tag{2.3.7}$$

where Eq. (2.3.2) was used. If we substitute $\bar{n}$ from Eq. (2.2.43) and use Eq. (2.2.35), $D$ can be written as the sum of two terms,

$$D = D_M + D_W, \tag{2.3.8}$$

where the *material dispersion* $D_M$ and the *waveguide dispersion* $D_W$ are given by

$$D_M = -\frac{2\pi}{\lambda^2}\frac{dn_{2g}}{d\omega} = \frac{1}{c}\frac{dn_{2g}}{d\lambda}, \tag{2.3.9}$$

$$D_W = -\frac{2\pi\Delta}{\lambda^2}\left[\frac{n_{2g}^2}{n_2\omega}\frac{Vd^2(Vb)}{dV^2} + \frac{dn_{2g}}{d\omega}\frac{d(Vb)}{dV}\right]. \tag{2.3.10}$$

Here $n_{2g}$ is the group index of the cladding material and the parameters $V$ and $b$ are given by Eqs. (2.2.35) and (2.2.36), respectively. In obtaining Eqs. (2.3.8)–(2.3.10) the parameter $\Delta$ was assumed to be frequency independent. A third term known as differential material dispersion should be added to Eq. (2.3.8) when $d\Delta/d\omega \neq 0$. Its contribution is, however, negligible in practice.

### 2.3.2 Material Dispersion

Material dispersion occurs because the refractive index of silica, the material used for fiber fabrication, changes with the optical frequency $\omega$. On a fundamental level, the origin of material dispersion is related to the characteristic resonance frequencies at which the material absorbs the electromagnetic radiation. Far from the medium resonances, the refractive index $n(\omega)$ is well approximated by the *Sellmeier equation* [33]

$$n^2(\omega) = 1 + \sum_{j=1}^{M}\frac{B_j\omega_j^2}{\omega_j^2 - \omega^2}, \tag{2.3.11}$$

where $\omega_j$ is the resonance frequency and $B_j$ is the oscillator strength. Here $n$ stands for $n_1$ or $n_2$, depending on whether the dispersive properties of the core or the cladding are considered. The sum in Eq. (2.3.11) extends over all material resonances that contribute in the frequency range of interest. In the case of optical fibers, the parameters $B_j$ and $\omega_j$ are obtained empirically

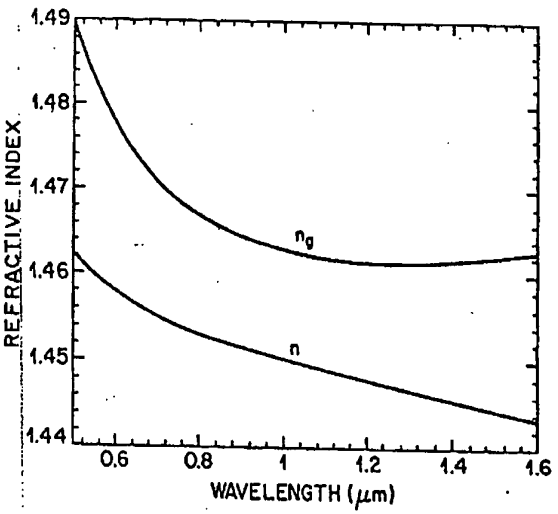


**Figure 2.8** Variation of refractive index $n$ and group index $n_g$ with wavelength for fused silica.

by fitting the measured dispersion curves to Eq. (2.3.11) with $M = 3$. They depend on the amount of dopants and have been tabulated for several kinds of fibers [12]. For pure silica these parameters are found to be $B_1 = 0.6961663$, $B_2 = 0.4079426$, $B_3 = 0.8974794$, $\lambda_1 = 0.0684043\ \mu$m, $\lambda_2 = 0.1162414\ \mu$m, and $\lambda_3 = 9.896161\ \mu$m, where $\lambda_j = 2\pi c/\omega_j$ with $j = 1$–3 [33]. The group index $n_g = n + \omega(dn/d\omega)$ can be obtained by using these parameter values.

Figure 2.8 shows the wavelength dependence of $n$ and $n_g$ in the range 0.5–1.6 $\mu$m for fused silica. Material dispersion $D_M$ is related to the slope of $n_g$ by the relation $D_M = c^{-1}(dn_g/d\lambda)$ [Eq. (2.3.9)]. It turns out that $dn_g/d\lambda = 0$ at $\lambda = 1.276\ \mu$m. This wavelength is referred to as the *zero-dispersion wavelength* $\lambda_{ZD}$, since $D_M = 0$ at $\lambda = \lambda_{ZD}$. The dispersion parameter $D_M$ is negative below $\lambda_{ZD}$ and becomes positive above that. In the wavelength range 1.25–1.66 $\mu$m it can be approximated by an empirical relation

$$D_M \approx 122(1 - \lambda_{ZD}/\lambda). \tag{2.3.12}$$

It should be stressed that $\lambda_{ZD} = 1.276\ \mu$m only for pure silica. It can vary in the range 1.27–1.29 $\mu$m for optical fibers whose core and cladding are doped to vary the refractive index. The zero-dispersion wavelength of optical fibers also depends on the core radius $a$ and the index step $\Delta$ through the waveguide contribution to the total dispersion.

### 2.3.3 Waveguide Dispersion

The contribution of waveguide dispersion $D_W$ to the dispersion parameter $D$ is given by Eq. (2.3.10) and depends on the $V$ parameter of the fiber. Figure 2.9



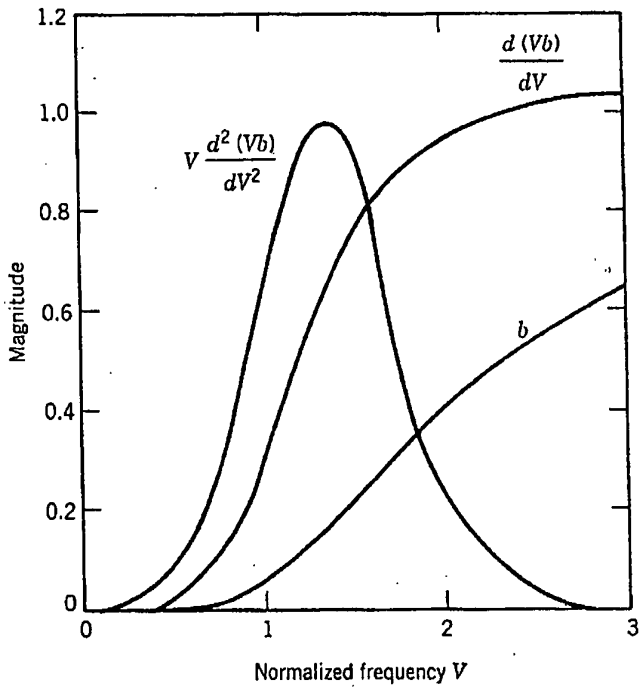


**Figure 2.9** Variation of $b$ and its derivatives $d(Vb)/dV$ and $V[d^2(Vb)/dV^2]$ with the $V$ parameter. (After Ref. [30]. ©1971 OSA. Reprinted with permission.)

shows how $d(Vb)/dV$ and $Vd^2(Vb)/dV^2$ change with $V$. Since both derivatives are positive, $D_W$ is negative in the entire wavelength range 0–1.6 $\mu$m. On the other hand, $D_M$ is negative for wavelengths below $\lambda_{ZD}$ and becomes positive above that. Figure 2.10 shows $D_M$, $D_W$, and their sum $D = D_M + D_W$, for a typical single-mode fiber. The main effect of waveguide dispersion is to shift $\lambda_{ZD}$ by an amount 30–40 nm so that the total dispersion is zero near 1.31 $\mu$m. It also reduces $D$ from its material value $D_M$ in the wavelength range 1.3–1.6 $\mu$m that is of interest for optical communication systems. Typical values of $D$ are in the range 15–18 ps/(km-nm) near 1.55 $\mu$m. This wavelength region is of considerable interest for lightwave systems, since, as discussed in Section 2.5, the fiber loss is minimum near 1.55 $\mu$m. High values of $D$ limit the performance of 1.55-$\mu$m lightwave systems.

Since the waveguide contribution $D_W$ depends on fiber parameters such as the core radius $a$ and the index difference $\Delta$, it is possible to design the fiber such that $\lambda_{ZD}$ is shifted into the vicinity of 1.55 $\mu$m [34], [35]. Such fibers are called *dispersion-shifted fibers*. It is also possible to tailor the waveguide contribution such that the total dispersion $D$ is relatively small over a wide wavelength range extending from 1.3 to 1.6 $\mu$m [36]–[38]. Such fibers are called *dispersion-flattened*

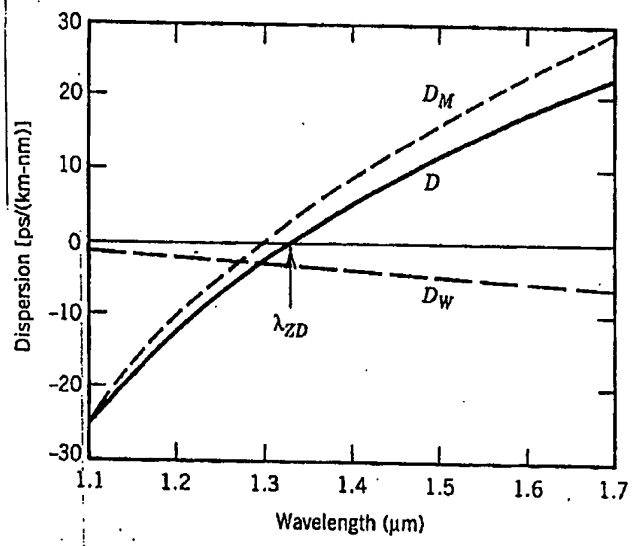


**Figure 2.10** Total dispersion $D$ and relative contributions of material dispersion $D_M$ and waveguide dispersion $D_W$ for a conventional single-mode fiber. The zero-dispersion wavelength shifts to a higher value because of the waveguide contribution.

*fibers*. Figure 2.11 shows typical examples of the wavelength dependence of $D$ for standard (conventional), dispersion-shifted, and dispersion-flattened fibers. The design of dispersion-modified fibers involves the use of multiple cladding layers and a tailoring of the refractive-index profile [34]–[40]. Design issues are discussed in Section 2.7. Table 2.1 lists the operating characteristics of several commercially available fibers having minimum dispersion near 1.3- and 1.55-$\mu$m wavelengths. Since 1991, waveguide dispersion has been used to produce fibers whose GVD decreases along the fiber length through axial variations in the core radius. Such fibers, called *dispersion-decreasing fibers*, have found applications in the context of solitons (see Chapter 10).

**Table 2.1 Characteristics of several commercial fibers**

| Fiber Type | NA | $\Delta$ (%) | $2w$ ($\mu$m) | $\lambda_{ZD}$ ($\mu$m) | GVD Slope $S$ [ps/(km-nm$^2$)] |
|---|---|---|---|---|---|
| Corning SMF-28 | 0.13 | 0.36 | 9.3 | 1.312 | 0.090 |
| AT&T Matched-Clad | 0.12 | 0.33 | 9.3 | 1.312 | 0.088 |
| LITESPEC GSM-13 | 0.12 | 0.33 | 9.3 | 1.312 | 0.087 |
| Corning SMF-DS | 0.17 | 0.90 | 8.1 | 1.550 | 0.075 |
| AT&T TrueWave | 0.16 | 0.75 | 8.4 | 1.530 | 0.095 |
| LITESPEC DSM-15 | 0.17 | 0.90 | 8.0 | 1.555 | 0.072 |



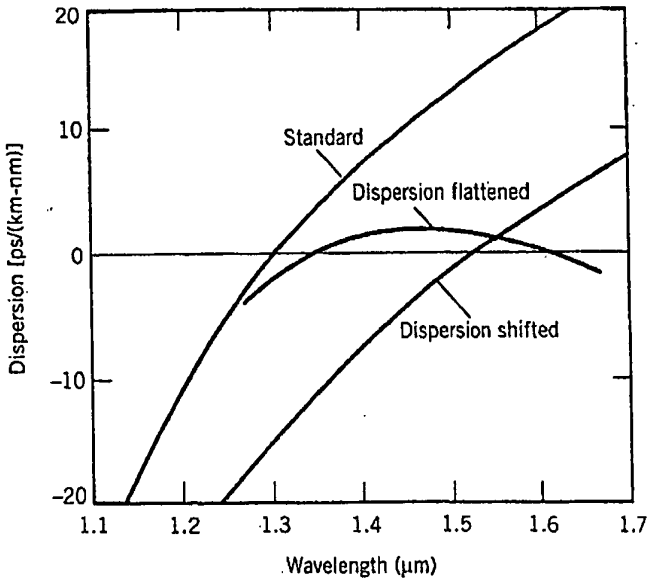


**Figure 2.11** Typical wavelength dependence of the dispersion parameter $D$ for standard, dispersion-shifted, and dispersion-flattened fibers.

### 2.3.4 Higher-Order Dispersion

It appears from Eq. (2.3.6) that the $BL$ product of a single-mode fiber can be increased indefinitely by operating at the zero-dispersion wavelength $\lambda_{ZD}$ where $D = 0$. The dispersive effects, however, do not disappear completely at $\lambda = \lambda_{ZD}$. Optical pulses still experience broadening because of higher-order dispersive effects. This feature can be understood by noting that $D$ cannot be made zero at all wavelengths contained within the pulse spectrum centered at $\lambda_{ZD}$. Clearly, the wavelength dependence of $D$ will play a role in pulse broadening. Higher-order dispersive effects are governed by the *dispersion slope* $S = dD/d\lambda$. The parameter $S$ is also called a *differential-dispersion parameter* or *second-order dispersion parameter*. By using Eq. (2.3.5) it can be written as

$$S = (2\pi c/\lambda^2)^2\beta_3 + (4\pi c/\lambda^3)\beta_2\,, \tag{2.3.13}$$

where $\beta_3 = d\beta_2/d\omega = d^3\beta/d\omega^3$. At $\lambda = \lambda_{ZD}$, $\beta_2 = 0$, and $S$ is proportional to $\beta_3$. Typical values of $S$ at $\lambda = \lambda_{ZD}$ are listed in Table 2.1 for both standard and dispersion-shifted fibers. For a source of spectral width $\Delta\lambda$, the effective value of dispersion parameter becomes $D = S\Delta\lambda$. The limiting bit rate–distance product can be estimated by using Eq. (2.3.6) with this value of $D$, or by using

$$BL|S|(\Delta\lambda)^2 < 1\,. \tag{2.3.14}$$

For a multimode semiconductor laser with $\Delta\lambda = 2$ nm and a dispersion-shifted fiber with $S = 0.05$ ps/(km-nm$^2$) at $\lambda = 1.55$ $\mu$m, the $BL$ product can ap-

proach 5 (Tb/s)-km. Further improvement is possible by using single-mode semiconductor lasers.

### 2.3.5 Polarization-Mode Dispersion

A potential source of pulse broadening is related to fiber birefringence. As discussed in Section 2.2.3, small departures from perfect cylindrical symmetry lead to birefringence because of different mode indices associated with the orthogonally polarized components of the fundamental fiber mode. If the input pulse excites both polarization components, it becomes broader at the fiber output since the two components disperse along the fiber because of their different group velocities. This phenomenon, referred to as *polarization-mode dispersion* (PMD), has been studied extensively during the 1990s because of its importance for periodically amplified lightwave systems [41]–[47].

Similar to the case of GVD, pulse broadening can be estimated from the time delay $\Delta T$ between the two polarization components during propagation of the pulse. For a fiber of length $L$, $\Delta T$ is given by

$$\Delta T = \left| \frac{L}{v_{gx}} - \frac{L}{v_{gy}} \right| = L|\beta_{1x} - \beta_{1y}| = L\Delta\beta_1, \tag{2.3.15}$$

where the subscripts $x$ and $y$ identify the two orthogonally polarized modes and $\Delta\beta_1$ is related to the fiber birefringence. Equation (2.3.1) was used to relate the group velocity $v_g$ to the propagation constant $\beta$. Similar to the case of intermodal dispersion discussed in Section 2.1.1, the quantity $\Delta T/L$ is a measure of PMD. For polarization-preserving fibers, $\Delta T/L$ is quite large ($\sim 1$ ns/km) when the two components are equally excited at the fiber input but can be reduced to zero by launching light along one of the principal axes.

Equation (2.3.15) cannot be used directly to estimate PMD for standard telecommunication fibers because of random coupling between the two modes, induced by random perturbations of birefringence occurring along the fiber. The coupling tends to equalize the propagation times for the two polarization components. In fact, PMD is characterized by the root-mean-square (RMS) value of $\Delta T$ obtained after averaging over random perturbations. The result is found to be [42], [46]

$$\sigma_T^2 = \langle (\Delta T)^2 \rangle = \frac{1}{2}\Delta\beta_1^2 h^2 \left[ \frac{2L}{h} - 1 + \exp\left( -\frac{2L}{h} \right) \right]. \tag{2.3.16}$$

where $h$ is the decorrelation length, with typical values in the range 1–10 m [47]. For polarization-preserving fibers, the decorrelation length is infinitely large, and the PMD $\sigma_T$ increases linearly with the fiber length, as expected. In contrast, for $h \ll L$,

$$\sigma_T \approx \Delta\beta_1 \sqrt{hL} = D_p \sqrt{L}, \tag{2.3.17}$$

where $D_p$ is the PMD parameter with typical values in the range $D_p = 0.1$–$1$ ps/$\sqrt{\text{km}}$. Because of its $\sqrt{L}$ dependence, PMD-induced pulse broadening is relatively small compared with the GVD effects. However, PMD can become a limiting factor for fiber-optic communication systems designed to operate over long distances near the zero-dispersion wavelength of the fiber [44], [45].



## 2.4 DISPERSION-INDUCED LIMITATIONS

Pulse broadening, discussed in Section 2.3.1 [see Eq. (2.3.4)], is based on an intuitive phenomenological approach. It provides a first-order estimate for pulses whose spectral width is dominated by the spectrum of the optical source rather than by the Fourier spectrum of the pulse. In general, the extent of pulse broadening depends on the width and the shape of the input pulse. In this section we discuss pulse broadening by using the wave equation (2.2.16).

### 2.4.1 Basic Propagation Equation

The discussion of fiber modes in Section 2.2.2 showed that each frequency component of the optical field propagates in a single-mode fiber as

$$\tilde{\mathbf{E}}(\mathbf{r},\omega) = \hat{\mathbf{x}} F(x,y) \tilde{B}(0,\omega) \exp(i\beta z), \tag{2.4.1}$$

where $\hat{\mathbf{x}}$ is the polarization unit vector, $\tilde{B}(0,\omega)$ is the initial amplitude, and $\beta$ is the propagation constant. $F(x,y)$ is the field distribution of the fundamental fiber mode that can often be approximated by a Gaussian distribution [see Eq. (2.2.45)]. In general, $F(x,y)$ also depends on $\omega$, but this dependence can be ignored for pulses whose spectral width $\Delta\omega \ll \omega_0$, a condition generally satisfied in practice. Here $\omega_0$ is the frequency at which the pulse spectrum is centered; it is referred to as the center frequency or carrier frequency. Different spectral components propagate inside the fiber according to the simple relation

$$\tilde{B}(z,\omega) = \tilde{B}(0,\omega) \exp(i\beta z). \tag{2.4.2}$$

The amplitude in the time domain can be obtained by taking the inverse Fourier transform and is given by

$$B(z,t) = \frac{1}{2\pi} \int_{-\infty}^{\infty} \tilde{B}(z,\omega) \exp(-i\omega t)\, d\omega. \tag{2.4.3}$$

The initial spectral amplitude $\tilde{B}(0,\omega)$ is just the Fourier transform of the input amplitude $B(0,t)$.

Pulse broadening results from the frequency dependence of $\beta$. For quasi-monochromatic pulses with $\Delta\omega \ll \omega_0$, it is useful to expand $\beta(\omega)$ in a Taylor series around the carrier frequency $\omega_0$ and retain terms up to third order, that is,

$$\beta(\omega) = \bar{n}(\omega)\frac{\omega}{c} \approx \beta_0 + \beta_1(\Delta\omega) + \frac{1}{2}\beta_2(\Delta\omega)^2 + \frac{1}{6}\beta_3(\Delta\omega)^3, \tag{2.4.4}$$

where $\Delta\omega = \omega - \omega_0$ and $\beta_m = (d^m\beta/d\omega^m)_{\omega=\omega_0}$. From Eq. (2.3.1) $\beta_1 = 1/v_g$, where $v_g$ is the group velocity. The GVD coefficient $\beta_2$ is related to the dispersion parameter $D$ by Eq. (2.3.5), whereas $\beta_3$ is related to the dispersion

# 10.1 FIBER SOLITONS

The existence of fiber solitons is the result of a balance between *group-velocity dispersion* (GVD) and *self-phase modulation* (SPM), both of which, as discussed in Sections 2.4 and 5.2, limit the performance of fiber-optic communication systems when acting independently on optical pulses propagating inside the fiber. One can develop an intuitive understanding of how such a balance is possible by following the analysis of Section 2.4. As shown there, the GVD broadens optical pulses during their propagation inside the fiber except when the pulse is initially chirped in the right way (see Fig. 2.12). More specifically, a chirped pulse can be compressed during the early stage of propagation whenever the GVD parameter $\beta_2$ and the chirp parameter $C$ happen to have opposite signs, so that $\beta_2 C$ is negative. SPM, resulting from the intensity dependence of the refractive index, imposes a chirp on the optical pulse such that $C > 0$. Since $\beta_2 < 0$ in the 1.55-$\mu$m wavelength region, the condition $\beta_2 C < 0$ is readily satisfied. Moreover, since the SPM-induced chirp is power dependent, it is not difficult to imagine that under certain conditions, SPM and GVD may cooperate in such a way that the SPM-induced chirp is just right to cancel the GVD-induced broadening of the pulse. The optical pulse would then propagate undistorted in the form of a soliton.

## 10.1.1 Nonlinear Schrödinger Equation

The mathematical description of fiber solitons requires solution of the wave equation in a dispersive nonlinear medium. A simple approach is to start with the propagation equation [Eq. (2.4.7)], satisfied by the slowly varying pulse envelope $A(z,t)$ in the presence of GVD, and modify it to include the effects of fiber nonlinearity responsible for SPM. Equation (2.6.5) provides a clue for such a modification. Since silica fibers are only weakly nonlinear (the intensity-dependent change in the refractive index is typically $< 10^{-9}$), the effect of SPM can be included by adding a nonlinear term on the right side of Eq. (2.4.7) so that this equation takes the form [6]

$$\frac{\partial A}{\partial z} + \beta_1 \frac{\partial A}{\partial t} + \frac{i}{2}\beta_2 \frac{\partial^2 A}{\partial t^2} - \frac{1}{6}\beta_3 \frac{\partial^3 A}{\partial t^3} = i\gamma |A|^2 A - \frac{\alpha}{2} A, \tag{10.1.1}$$

where the fiber loss is included through $\alpha$, $\beta_1 = v_g^{-1}$ with $v_g$ representing the group velocity, $\beta_2$ and $\beta_3$ account for fiber dispersion, and $\gamma$ is the nonlinearity parameter defined as

$$\gamma = 2\pi n_2 / \lambda A_{\text{eff}}. \tag{10.1.2}$$

Here $n_2$ is the nonlinear-index coefficient, $\lambda$ is the optical wavelength, and $A_{\text{eff}}$ is the *effective core area* introduced in Section 2.6.2 (the bars over $\gamma$ and $n_2$ appearing there are dropped for notational simplicity). The parameters $\beta_2$ and $\gamma$ govern the effects of GVD and SPM, respectively. Equation (10.1.1) is quite accurate for describing evolution of optical pulses as short as 5 ps. For pulses shorter than that, several higher-order nonlinear effects, discussed later in Section 10.4, need to be included [6]. Equation (10.1.1) can be used in most cases of practical interest.



To discuss soliton solutions of Eq. (10.1.1), we first set $\alpha = 0$ and $\beta_3 = 0$. The fiber loss is included later in Section 10.3, while the effects of third-order dispersion (TOD) are considered in Section 10.4. It is useful to write Eq. (10.1.1) in a normalized form by introducing

$$\tau = \frac{t - \beta_1 z}{T_0}, \qquad \xi = \frac{z}{L_D}, \qquad U = \frac{A}{\sqrt{P_0}}, \tag{10.1.3}$$

where $T_0$ is a measure of the pulse width, $P_0$ is the peak power of the pulse, and the dispersion length $L_D$ is defined as

$$L_D = T_0^2 / |\beta_2|. \tag{10.1.4}$$

Equation (10.1.1) then takes the form

$$i\frac{\partial U}{\partial \xi} - \text{sgn}(\beta_2)\frac{1}{2}\frac{\partial^2 U}{\partial \tau^2} + N^2 |U|^2 U = 0, \tag{10.1.5}$$

where $\text{sgn}(\beta_2) = +1$ or $-1$, depending on whether $\beta_2$ is positive (normal GVD) or negative (anomalous GVD). The parameter $N$ is defined by

$$N^2 = \gamma P_0 L_D = \gamma P_0 T_0^2 / |\beta_2|. \tag{10.1.6}$$

It represents a dimensionless combination of the pulse and fiber parameters. It will be seen later that $N$ has a physical significance. Equation (10.1.5) is known in the soliton literature [8]–[11] as the *nonlinear Schrödinger equation* (NSE).

## 10.1.2 Fundamental and Higher-Order Solitons

The NSE belongs to a special class of nonlinear partial differential equations that can be solved exactly by using a mathematical technique known as the *inverse scattering method* [8]–[10]. Although the NSE supports solitons for both normal and anomalous GVD, pulselike solitons are found only for the case of anomalous dispersion [12]. In the case of normal dispersion ($\beta_2 > 0$), the solutions occur in the form of a dip in a constant background. Such solutions, referred to as dark solitons, are discussed in Section 10.1.3. This chapter focuses on pulselike (bright) solitons since they are used almost exclusively for optical communications.

It is common to introduce $u = NU$ as a renormalized amplitude and write Eq. (10.1.5) in its canonical form as

$$i\frac{\partial u}{\partial \xi} + \frac{1}{2}\frac{\partial^2 u}{\partial \tau^2} + |u|^2 u = 0, \tag{10.1.7}$$

where $\beta_2 < 0$ was assumed. This equation has been solved by the inverse scattering method [12]. Details of this method are available in several books